

extraction. Copy number of mtDNA (ND1) was quantified by real-time polymerase chain reaction (PCR) using SYBR Green PCR Kit (Qiagen) with *pcam1* as the control for the nuclear genome copy number. We used the following primers: ND1 forward primer, CCTATCACCTTGCCATCAT; ND1 reverse primer, GAGGCTGTTGCTTGTGTGAC; *pcam1* DNA forward primer, ATGGAAAGCCTGCCATCATG; *pcam1* DNA reverse primer, TCCTTGTTGTTTCAGCATCAC.

The amount of mtDNA relative to nuclear DNA was calculated using the following formula: $\text{mtDNA/nuclear DNA} = 2^{-(C_{\text{mtDNA}} - C_{\text{nuclearDNA}})}$ where Ct is the threshold cycle (22).

Morphometrical analysis of mitochondria

Cross-sectional EM image of extensor digitorum longus (EDL) muscle from *rmd* and littermates was analyzed by Image J software (23). Total areas of all mitochondria in 20 muscle fibers were calculated and compared with cross-sectional fiber areas. Total number of mitochondria per muscle fiber was counted.

Antibodies

Primary antibodies used were: mouse anti-4-hydroxy-2-nonenal (4-HNE) modified protein antibody (HNEJ-2, JalCA), rabbit anti-PINK1 antibody (BC100-494, Novus Biologicals), mouse anti-Parkin antibody (4211, Cell Signaling), rabbit anti-p62/SQSTM1 antibody (PWS860, Biomol), rabbit anti-LC3 antibody (NB100-2220, Novus Biologicals), mouse anti-poly-ubiquitin antibody (FK1, Biomol), rabbit anti-TOM20 antibody (FL-145, Santa Cruz), mouse anti-COX subunit 1 antibody (Invitrogen) and mouse anti-VDAC antibody (20B12, Santa Cruz). Second antibodies used were: horse radish peroxidase-labeled goat anti-mouse (Beckman Coulter) or rabbit antibodies (Cell Signaling), Alexa Fluor 488- and Alexa Fluor 568-labeled goat anti-mouse or rabbit antibodies (Invitrogen).

Statistical analysis

Data are presented as mean \pm SD. Mean differences were compared with the analysis of *t*-test using R software version 2.11.0 (<http://www.r-project.org/>).

SUPPLEMENTARY MATERIAL

Supplementary Material is available at *HMG* online.

ACKNOWLEDGEMENTS

We thank Megumu Ogawa, Kanako Goto and Junko Takei for technical assistance.

FUNDING

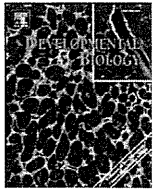
This study was supported partly by the Research on Psychiatric and Neurological Diseases and Mental Health of Health and Labour Sciences Research Grants; partly by the Research on Intractable Diseases of Health and Labor Sciences

Research Grants; partly by the Research Grant for Nervous and Mental Disorders (20B-12, 20B-13) from the Ministry of Health, Labour and Welfare; partly by an Intramural Research Grant (23-4, 23-5) for Neurological and Psychiatric Disorders from NCNP; partly by KAKENHI (20390250, 22791019); partly by Research on Publicly Essential Drugs and Medical Devices of Health and Labor Sciences Research Grants; partly by the Program for Promotion of Fundamental Studies in Health Sciences of the National Institute of Biomedical Innovation (NIBIO); and partly by the Grant from Japan Foundation for Neuroscience and Mental Health. G.A.C. and R.B.S. were supported in part by a National Institutes of Health Grant (AR054170 to G.A.C.).

REFERENCES

- Mitsuhashi, S., Ohkuma, A., Talim, B., Karahashi, M., Koumura, T., Aoyama, C., Kurihara, M., Quinlivan, R., Sewry, C., Mitsuhashi, H. *et al.* (2011) A congenital muscular dystrophy with mitochondrial structural abnormalities caused by defective de novo phosphatidylcholine biosynthesis. *Am. J. Hum. Genet.*, **88**, 845–851.
- Sher, R.B., Aoyama, C., Huebsch, K.A., Ji, S., Kerner, J., Yang, Y., Frankel, W.A., Hoppel, C.A., Wood, P.A., Vance, D.E. *et al.* (2006) A rostrocaudal muscular dystrophy caused by a defect in choline kinase beta, the first enzyme in phosphatidylcholine biosynthesis. *J. Biol. Chem.*, **281**, 4938–4948.
- Saraste, M. (1999) Oxidative phosphorylation at the fin de siècle. *Science*, **283**, 1488–1493.
- Spierings, D., McStay, G., Saleh, M., Bender, C., Chipuk, J., Maurer, U. and Green, D.R. (2005) Connected to death: the (unexpurgated) mitochondrial pathway of apoptosis. *Science*, **310**, 66–67.
- Wakabayashi, T. (2002) Megamitochondria formation—physiology and pathology. *J. Cell Mol. Med.*, **6**, 497–538.
- Benard, G., Bellance, N., James, D., Parrone, P., Fernandez, H. and Letellier, T. (2007) Mitochondrial bioenergetics and structural network organization. *J. Cell Sci.*, **120**, 838–848.
- Yoon, Y.S., Yoon, D.S., Lim, I.K., Yoon, S.H., Chung, H.Y., Rojo, M., Malka, F., Jou, M.J., Martinou, J.C. and Yoon, G. (2006) Formation of elongated giant mitochondria in DFO-induced cellular senescence: involvement of enhanced fusion process through modulation of Fis1. *J. Cell Physiol.*, **209**, 468–480.
- Karbowski, M., Kurono, C., Wozniak, M., Ostrowski, M., Teranishi, M., Nishizawa, Y., Usukura, J., Soji, T. and Wakabayashi, T. (1999) Free radical-induced megamitochondria formation and apoptosis. *Free Radic. Biol. Med.*, **26**, 396–409.
- Chen, H., Detmer, S.A., Ewald, A.J., Griffin, E.E., Fraser, S.E. and Chan, D.C. (2003) Mitofusins Mfn1 and Mfn2 coordinately regulate mitochondrial fusion and are essential for embryonic development. *J. Cell Biol.*, **160**, 189–200.
- Chen, H., Chomyn, A. and Chan, D.C. (2005) Disruption of fusion results in mitochondrial heterogeneity and dysfunction. *J. Biol. Chem.*, **280**, 26185–26192.
- Wu, G., Sher, R.B., Cox, G.A. and Vance, D.E. (2009) Understanding the muscular dystrophy caused by deletion of choline kinase beta in mice. *Biochim. Biophys. Acta*, **1791**, 347–356.
- Daum, G. (1985) Lipids of mitochondria. *Biochim. Biophys. Acta*, **822**, 1–42.
- Hayashi, Y.K., Matsuda, C., Ogawa, M., Goto, K., Tominaga, K., Mitsuhashi, S., Park, Y.E., Nonaka, I., Hino-Fukuyo, N., Haginoya, K. *et al.* (2009) Human PTRF mutations cause secondary deficiency of caveolins resulting in muscular dystrophy with generalized lipodystrophy. *J. Clin. Invest.*, **119**, 2623–2633.
- Bligh, E.G. and Dyer, W.J. (1959) A rapid method of total lipid extraction and purification. *Can. J. Biochem. Physiol.*, **37**, 911–917.
- Rouser, G., Fkeischer, S. and Yamamoto, A. (1970) Two dimensional thin layer chromatographic separation of polar lipids and determination of phospholipids by phosphorus analysis of spots. *Lipids*, **5**, 494–496.
- Mimaki, M., Hatakeyama, H., Ichiyama, T., Isumi, H., Furukawa, S., Akasaka, M., Kamei, A., Komaki, H., Nishino, I., Nonaka, I. *et al.* (2009)

- Different effects of novel mtDNA G3242A and G3244A base changes adjacent to a common A3243G mutation in patients with mitochondrial disorders. *Mitochondrion*, **9**, 115–122.
17. Trounce, I.A., Kim, Y.L., Jun, A.S. and Wallace, D.C. (1996) Assessment of mitochondrial oxidative phosphorylation in patient muscle biopsies, lymphoblasts, and transmittochondrial cell lines. *Methods enzymol.*, **264**, 484–509.
 18. Vives-Bauza, C., Yang, L. and Manfredi, G. *Methods in Cell Biology. Mitochondria*, 2nd edn. Academic Press, London, UK, Vol. 80, Part 2, 7, 155–171.
 19. Tang, P.H., Miles, M.V., Miles, L., Quinlan, J., Wong, B., Wensch, A. and Bove, K. (2004) Measurement of reduced and oxidized coenzyme Q9 and coenzyme Q10 levels in mouse tissues by HPLC with coulometric detection. *Clin. Chim. Acta*, **341**, 173–184.
 20. Wittig, I., Karas, M. and Schagger, H. (2007) High resolution clear native electrophoresis for in-gel functional assays and fluorescence studies of membrane protein complexes. *Mol. Cell Proteomics*, **6**, 1215–1225.
 21. Armstrong, J.S. and Whiteman, M. *Methods in Cell Biology. Mitochondria*, 2nd edn. Academic Press, London, UK, Vol. 80, 18, 355–377.
 22. Naini, A. and Shanske, S. *Methods in Cell Biology. Mitochondria*, 2nd edn. Academic Press, London, UK, Vol. 80, Part2, 22, 448–449.
 23. Abramoff, M.D., Magelhaes, P.J. and Ram, S.J. (2004) Image processing with Image J. *Biophotonics Int.*, **11**, 36–42.
 24. Zhang, M., Miletykovskaya, E. and Dowhan, W. (2002) Gluing the respiratory chain together. Cardiolipin is required for supercomplex formation in the inner mitochondrial membrane. *J. Biol. Chem.*, **277**, 43553–43556.
 25. Geisler, S., Holmström, K.M., Skujat, D., Fiesel, F.C., Rothfuss, O.C., Kahle, P.J. and Springer, W. (2010) PINK1/Parkin-mediated mitophagy is dependent on VDAC1 and p62/SQSTM1. *Nat. Cell Biol.*, **12**, 119–131.
 26. Narendra, D., Tanaka, A., Suen, D.F. and Youle, R.J. (2008) Parkin is recruited selectively to impaired mitochondria and promotes their autophagy. *J. Cell Biol.*, **183**, 795–803.
 27. Lee, A.G. (2003) Lipid-protein interactions in biological membranes: a structural perspective. *Biochim. Biophys. Acta*, **1612**, 1–40.
 28. Lange, C., Nett, J.H., Trumpower, B.L. and Hunte, C. (2001) Specific roles of protein-phospholipid interactions in the yeast cytochrome bcl complex structure. *EMBO J.*, **20**, 6591–6600.
 29. Hagopian, K., Weber, K.L., Hwee, D.T., Van Eenennaam, A.L., López-Lluch, G., Villalba, J.M., Burón, I., Navas, P., German, J.B., Watkins, S.M. *et al.* (2010) Complex I-associated hydrogen peroxide production is decreased and electron transport chain enzyme activities are altered in n-3 enriched fat-1 mice. *PLoS ONE*, **5**, e12696.
 30. Balaban, R.S., Nemoto, S. and Finkel, T. (2005) Mitochondria, oxidants, and aging. *Cell*, **120**, 483–495.
 31. St-Pierre, J., Buckingham, J.A., Roebeck, S.J. and Brand, M.D. (2002) Topology of superoxide production from different sites in the mitochondrial electron transport chain. *J. Biol. Chem.*, **277**, 44784–44790.
 32. Osaki, Y., Nishino, I., Murakami, N., Matsubayashi, K., Tsuda, K., Yokoyama, Y.I., Morita, M., Onishi, S., Goto, Y.I. and Nonaka, I. (1998) Mitochondrial abnormalities in selenium-deficient myopathy. *Muscle Nerve*, **21**, 637–639.
 33. Hill, K.E., Motley, A.K., Li, X., May, J.M. and Burk, R.F. (2001) Combined selenium and vitamin E deficiency causes fatal myopathy in guinea pigs. *J. Nutr.*, **131**, 1798–1802.
 34. Rederstorff, M., Krol, A. and Lescure, A. (2006) Understanding the importance of selenium and selenoproteins in muscle function. *Cell Mol. Life Sci.*, **63**, 52–59.
 35. Martensson, J. and Meister, A. (1989) Mitochondrial damage in muscle occurs after marked depletion of glutathione and is prevented by giving glutathione monoester. *Proc. Natl Acad. Sci. USA*, **86**, 471–475.
 36. Choksi, K.B., Boylston, W.H., Rabek, J.P., Widger, W.R. and Papaconstantinou, J. (2004) Oxidatively damaged proteins of heart mitochondrial electron transport complexes. *Biochim. Biophys. Acta*, **1688**, 95–101.
 37. Kim, I., Rodriguez-Enriquez, S. and Lemasters, J. (2007) Selective degradation of mitochondria by mitophagy. *Arch. Biochem. Biophys.*, **462**, 245–253.
 38. Tatsuta, T. and Langer, T. (2008) Quality control of mitochondria: protection against neurodegeneration and ageing. *EMBO J.*, **27**, 306–314.
 39. Ding, W.X., Ni, H.M., Li, M., Liao, Y., Chen, X., Stolz, D.B., Dorn, G.W. 2nd. and Yin, X.M. (2010) Nix is critical to two distinct phases of mitophagy, reactive oxygen species-mediated autophagy induction and Parkin-ubiquitin-p62-mediated mitochondrial priming. *J. Biol. Chem.*, **285**, 27879–27890.
 40. Moraes, C.T., Shanske, S., Tritschler, H.J., Aprille, J.R., Andreetta, F., Bonilla, E., Schon, E.A. and DiMauro, S. (1991) mtDNA depletion with variable tissue expression: a novel genetic abnormality in mitochondrial diseases. *Am. J. Hum. Genet.*, **48**, 492–501.
 41. Kim, I. and Lemasters, J.J. (2011) Mitochondrial degradation by autophagy (mitophagy) in GFP-LC3 transgenic hepatocytes during nutrient deprivation. *Am. J. Physiol. Cell Physiol.*, **300**, C308–C317.



Filamin C plays an essential role in the maintenance of the structural integrity of cardiac and skeletal muscles, revealed by the medaka mutant *zacro*

Misato Fujita^{a,1,2}, Hiroaki Mitsuhashi^{b,1}, Sumio Isogai^c, Takahiro Nakata^d, Atsushi Kawakami^a, Ikuya Nonaka^b, Satoru Noguchi^b, Yukiko K. Hayashi^b, Ichizo Nishino^b, Akira Kudo^{a,*}

^a Department of Biological Information, Tokyo Institute of Technology, 4259-B-33 Nagatsuta, Midori-ku, Yokohama 226-8501, Japan

^b Department of Neuromuscular Research, National Institute of Neuroscience, National Center of Neurology and Psychiatry, 4-1-1 Ogawa-higashi, Kodaira, Tokyo 187-8502, Japan

^c Department of Anatomy, School of Medicine, Iwate Medical University, 2-1-1 Nishitokuta, Yahaba, Shiwa 028-3694, Japan

^d Department of Health Science, Ishikawa Prefectural Nursing University, 1-1 Gakuendai, Kahoku, Ishikawa 929-1210, Japan

ARTICLE INFO

Article history:

Received for publication 19 July 2011

Revised 5 October 2011

Accepted 6 October 2011

Available online 14 October 2011

Keywords:

Medaka mutant

Filamin C

Cardiac muscle

Skeletal muscle

zacro

ABSTRACT

Filamin C is an actin-crosslinking protein that is specifically expressed in cardiac and skeletal muscles. Although mutations in the filamin C gene cause human myopathy with cardiac involvement, the function of filamin C *in vivo* is not yet fully understood. Here we report a medaka mutant, *zacro* (*zac*), that displayed an enlarged heart, caused by rupture of the myocardial wall, and progressive skeletal muscle degeneration in late embryonic stages. We identified *zac* to be a homozygous nonsense mutation in the *filamin C* (*finc*) gene. The medaka filamin C protein was found to be localized at myotendinous junctions, sarcolemma, and Z-disks in skeletal muscle, and at intercalated disks in the heart. *zac* embryos showed prominent myofibrillar degeneration at myotendinous junctions, detachment of myofibrils from sarcolemma and intercalated disks, and focal Z-disk destruction. Importantly, the expression of γ -actin, which we observed to have a strong subcellular localization at myotendinous junctions, was specifically reduced in *zac* mutant myotomes. Inhibition of muscle contraction by anesthesia alleviated muscle degeneration in the *zac* mutant. These results suggest that filamin C plays an indispensable role in the maintenance of the structural integrity of cardiac and skeletal muscles for support against mechanical stress.

© 2011 Elsevier Inc. All rights reserved.

Introduction

Skeletal muscle and heart are the organs that produce physical force by muscle contraction, and muscle fibers are incessantly exposed to strong mechanical stress. To protect intracellular structures against such mechanical stress, muscle fibers express a variety of muscle-specific proteins that often form large complexes.

Two major protein complexes, the dystrophin-associated glycoprotein complex (DGC) and the integrin complex are known to have important roles in affording mechanical integrity to striated muscle. In skeletal muscle, these complexes, which are localized at the sarcolemma (Arahata et al., 1988; Mayer, 2003; Watkins et al., 1988) and myotendinous junctions (MTJs; (Bao et al., 1993; Samitt and Bonilla, 1990; Shimizu et al., 1989), where the muscle fibers are connected to tendon, link the subsarcolemmal actin cytoskeleton to the extracellular matrix (ECM) (Burkin and Kaufman, 1999;

Campbell, 1995; Yoshida et al., 2000). Defects in the components of this DGC lead to muscular dystrophy (Bonnemann et al., 1995; Hoffman et al., 1987; Lim et al., 1995; Nigro et al., 1996; Noguchi et al., 1995; Roberds et al., 1994), an inherited muscular disorder characterized by progressive muscle degeneration, suggesting the importance of this linkage system for the integrity of muscle fibers. Muscle fibers specifically express $\alpha 7 \beta 1$ integrin, and a defect of $\alpha 7$ integrin causes muscular dystrophy, primarily affecting muscle fibers close to the MTJs (Hayashi et al., 1998; Mayer et al., 1997; Miosge et al., 1999), pointing to the importance of the integrin-based linkage for muscle integrity, particularly at MTJs. In heart, DGC and integrins are localized at the sarcolemma as well as at intercalated disks, which are the contact sites between cardiomyocytes (Anastasi et al., 2009; van der Flier et al., 1997).

The Z-disk is a huge multi-protein complex that constitutes the border of individual sarcomeres. This Z-disk plays a key role in the crosslinking of actin thin filaments of myofibrils to withstand the extreme mechanical force generated during muscle contraction. Z-disks are attached to the sarcolemmal DGC and integrin complexes at the sites of costameres via Z-disk-associated linker molecules (Ervasti, 2003). Recently, mutations in genes encoding Z-disk components have been found to be responsible for a group of muscle diseases termed myofibrillar myopathy, which is pathologically characterized by myofibrillar disorganization, including the degeneration of the

* Corresponding author. Fax: +81 45 924 5718.

E-mail address: akudo@bio.titech.ac.jp (A. Kudo).

¹ Misato Fujita and Hiroaki Mitsuhashi were equal contributors to this study.

² Present address. Section on Vertebrate Organogenesis, Program in Genomics of Differentiation, Eunice Kennedy Shriver National Institute of Child Health and Human Development, National Institutes of Health, MD 20892, USA.

sarcomere structure (Selcen, 2008; Selcen et al., 2004). These reports suggest that Z-disk proteins have important roles in maintaining organized sarcomere structures.

Filamins are actin-crosslinking proteins first purified by their ability to bind and precipitate actin (Hartwig and Stossel, 1975; Stossel and Hartwig, 1975). Filamins are composed of 3 isoforms, filamins A, B, and C. All filamins consist of an N-terminal actin-binding domain followed by 24 immunoglobulin-like repeats, and they dimerize at the 24th repeat domain located at the C-terminus (Stossel et al., 2001). Filamins directly interact with more than 30 diverse proteins, and are involved in multiple cellular processes including cell–cell and cell–matrix adhesion, mechanoprotection, actin remodeling, and various intracellular signaling pathways (Feng and Walsh, 2004). Filamin C is a muscle-specific isoform and localizes at MTJs, costameres, Z-disks, and intercalated disks in mammal and avian muscles (Ohashi et al., 2005; van der Ven et al., 2000a). Interestingly, filamin C interacts with both DGC (Thompson et al., 2000) and integrin (Gontier et al., 2005; Loo et al., 1998), as well as with the Z-disk proteins myotilin (van der Ven et al., 2000b), FATZ-1 (Faulkner et al., 2000), and myopodin (Linnemann et al., 2010) through its C-terminal region. Such localization and protein interaction suggest that filamin C functions in maintaining the mechanical integrity of muscle cells. Recently, mutations in the filamin C gene were identified in patients having myofibrillar myopathy (Kley et al., 2007; Luan et al., 2010; Shatunov et al., 2009; Vorgerd et al., 2005). These patients frequently develop cardiac abnormalities in addition to skeletal myopathy, suggesting the essential role of filamin C in both skeletal and cardiac muscles. To investigate the function of filamin C *in vivo*, Dalkilic et al. (2006) generated *filamin C*-deficient mice having a deletion of the last 8 exons of *FlnC*. This deficient mouse shows fewer muscle fibers or primary myotubes than normal and abnormal rounded fibers, suggesting defects in primary myogenesis; however, this mouse does not present any cardiac defects, which indicates a partial-loss-of-function. Since these mice die *in utero* or live only a short while after birth, further detailed observations cannot be carried out.

Recently, zebrafish have emerged as an alternative model organism to study the vertebrate muscular system and to isolate new dystrophy-causing genes/pathways (Guyon et al., 2007; Steffen et al., 2007). A deficiency of DGC or integrin-linked kinase causes a muscular dystrophic phenotype in zebrafish embryos (Bassett et al., 2003; Cheng et al., 2006; Gupta et al., 2011; Guyon et al., 2005; Postel et al., 2008), suggesting that their functions are likely to be analogous to those in humans. In zebrafish embryos, the DGC is localized initially at the junctional area, where the ends of muscle fibers attach to the myosepta, corresponding to the myotendinous junction (MTJ). Loss of DGC causes muscle fiber detachment at MTJs, indicating compromised adhesion between muscle fibers and the ECM of myosepta. Medaka (*Oryzias latipes*), another teleost fish, has the experimental advantages of external development, transparency, and quick production of a number of embryos, similar to the zebrafish. Unlike zebrafish, however, various medaka inbred strains have been established; and the medaka genome, which is about one-half of the size of the zebrafish genome, is almost fully sequenced and aligned, indicating that the medaka has powerful advantages for the application of forward genetics (Ishikawa, 2000; Wittbrodt et al., 2002).

Here, we identified a medaka mutant, *zacro* (*zac*), that has a nonsense mutation, resulting in an early truncation at the 15th immunoglobulin-like repeat of the medaka orthologue of filamin C. This mutation causes myocardial rupture in the ventricle. Although this mutant displayed normal myogenesis in myotome muscles during early stages of embryonic development, its myofibrils gradually degenerated and became disorganized in later stages. Detailed histological analysis suggests an indispensable role of filamin C in the maintenance of the muscle structure rather than in its formation in both heart and skeletal muscles.

Materials and methods

Medaka strains and mutant screening

All studies requiring wild-type medaka (*O. latipes*) were carried out by using the Qurt strain, which was derived from the southern population (Wada et al., 1998). Fish were maintained in an aquarium system with re-circulating water at 28.5 °C. Embryos were obtained from natural spawning, and incubated at 28 ± 2 °C. Stages were determined as previously described (Iwamatsu, 2004). *N*-ethyl-*N*-nitrosourea (ENU) was used for mutagenesis, and a standard genetic F3 screening for mutations affecting embryogenesis were performed as described earlier (Ishikawa, 1996; Ishikawa et al., 1999). The *zac* mutant was identified by microscopic inspection as a Mendelian-inherited recessive lethal mutation that caused a phenotype characterized by congestion in the blood vessels and pericardial edema.

Positional cloning

zac heterozygous fish, which were maintained on the southern Qurt genomic background, were mated with the northern HNI strain fish (Hyodo-Taguchi, 1980) to generate F1 families. Embryos for the genetic mapping were obtained from inter-crosses of F1 *zac* carriers. To locate the genetic linkage, we conducted bulk segregant analysis on pools of genomic DNA from *zac* mutants and wild-type embryos by using sequence tagged site (STS) markers on the medaka genome (Kimura et al., 2004). The *zac* region was narrowed down by using additional STS markers, AU171271 and Olb2110h (Naruse et al., 2000), and newly designed restriction fragment length polymorphism (RFLP) markers, HAL and KCND2 (HAL; 5'-GGATGGGCAGATGCCAAATATG-3' and 5'-GTCCCGTTGATCAGAGCCAG-3'/MboI, KCND2; 5'-CAGCAGGTGTAGCGGCATG-3' and 5'-GTTGGCCATCACTGATATGGC-3'/AfaI). cDNAs of *finc* from *zac* mutant and wild-type embryos were amplified, and verified by sequencing. The full-length cDNA of *finc* was cloned by PCR using primers including XbaI restriction enzyme sites [5'-CAATCTAGACAAG-GAACAAGCC-3' and 5'-GAATCTAGACCACCATTTAGCC-3'], and was sequenced. We obtained 2 different *finc* clones, which appeared to be splice variants. To confirm the linkage between the *zac* mutation and *finc* gene, we performed allele-specific PCR using 2 independent outer primers [5'-TTCAGTTGGAGGACATGGGAT-3' and 5'-GACACCTGCAACA-CAACTCTA-3'] in combination with either a wild type-specific antisense primer [5'-CTTGCAGGTCACCTTTCCTTT-3'] or a mutant-specific one [5'-CTTGCAGGTCACCTTTCCTTA-3']. We also performed 5'-RACE and 3'-RACE to obtain full-length sequence information on *finc* cDNA. The sequences of the medaka *finc* have been deposited in GenBank under the accession numbers AB639344 and AB639345.

Birefringence assay

Embryos were dechorionated at stage 27. Muscle birefringence was analyzed at stages 32 and 34 by placing anesthetized embryos on a glass dish and observing them with an underlit dissecting scope (Olympus, SZX12) having 2 polarizing filters (Olympus, SZX-P0 and SZX2-AN). The top polarizing filter was twisted until only the light refracting through the striated muscle was visible.

Histological analysis

Embryos were fixed overnight at 4 °C in 4% paraformaldehyde (PFA) in phosphate-buffered saline pH 7.4 (PBS), dehydrated by ethanol, and embedded in a resin (Technovit 8100, Kulzer Heraeus) according to the manufacturer's instructions. Sections were cut at 2 µm and stained with Harris's hematoxylin and Eosin Y or Masson trichrome staining buffer (SIGMA).

Whole-mount RNA *in situ* hybridization

Whole-mount RNA *in situ* hybridization was performed as previously described (Inohaya et al., 1995; Inohaya et al., 1999). Digoxigenin-labeled antisense RNA probes for cardiac myosin light chain 2 (*cmlc2*), desmin (*des*), *flnc*, *myf5*, *nkx2.5*, *tbx5a*, and ventricular myosin heavy chain (*vmhc*) were used. The primer sets used for cloning the respective probes are listed below.

cmlc2 F: AATGTCTTTTCCATGTTYGARC
 R: CAGATTCAGCAGTTAARGARG and CTCCTCTTTCATCHCCATG
des F: AACACCAGCCAACCATGAGC
 R: ACAGATGTAGTTATCCTGCAGG
flnc F: GCTCCAGAGGAAATTGTGGAC
 R: CTCACACCTTTAGGCTGTAGC
myf5 F: ATCCACTTCTTCTCCCGAGC
 R: TTTCTCTCAGAGAGAACC
nkx2.5 F: TTCTCTCAGGCGCAGGTGTACGAGC
 R: GCDGGGTAGGYGTTGTA
tbx5a F: GTCTGAGATTTCCGAGCTCC
 R: CTCTCTAGACTCGAGTTGGTCTTCTGTGTCTCC
vmhc F: GGAGCTGGATGATGTGGTTTC
 R: CATGGGCTAAGCGCTTCTTGGC
 (R: A,G,Y: C,T,H: A,C,T)

Injection of morpholino antisense oligonucleotide (MO)

We obtained a specific MO (Gene Tools) to interfere with *flnc* translation. The MO [5'-GGCCATCATGTTGGCTTGTCCCTTG-3'] was dissolved at concentrations from 100 to 1000 μ M in nuclease-free water. Approximately 0.5 nl of MO solution or standard control MO [5'-CCTCTTACTCAGTTACAATTATA-3'] was injected into 1-cell-stage embryos.

Whole-mount immunofluorescence

Dechorionated embryos were anesthetized in 0.02% tricaine methanesulfonate and fixed in 4% PFA in PBS at 4 °C overnight. We used chilled methanol at –20 °C as the fixative for anti-laminin antibody, and IHC Zinc fixative (BD Biosciences) for anti- γ -actin antibody. After fixation, embryos were dehydrated in a graded series of methanols (25–50–75%) and stored in 100% methanol at –20 °C. Embryos were rehydrated in a graded series of methanols (75–50–25%) and washed 3 times for 15 min each time in MABTr (0.1 M maleic acid and 150 mM NaCl containing 0.1% Triton X-100) and subsequently in MABDTr (MABTr with 1% BSA and 1% DMSO) twice for 30 min each time. Following blocking with 5% goat serum in MABDTr for 30 min, the embryos were incubated with primary antibodies at 4 °C overnight. The following antibodies were used: anti-filamin C (SIGMA HPA006135; 1:100), anti-vinculin (SIGMA V4505; 1:50), anti- α -actinin (SIGMA A7811; 1:500), anti-integrin β 1D (Millipore MAB1900; 1:25), anti- β -sarcoglycan (Novocastra NCL-b-SARC; 1:50), anti-slow muscle myosin heavy chain (F59, DSHB; 1:100), anti-FAK pY397 (Invitrogen 44-625G; 1:100), anti-dystrophin (SIGMA D8043; 1:100), anti- β -dystroglycan (Novocastra NCL-b-DG; 1:100), and anti-phospho-paxillin (Cell Signaling Technology #2541; 1:50). Rabbit polyclonal anti-cytoplasmic γ -actin antibody was previously characterized (Nakata et al., 2001), and used at a dilution of 1:100. Embryos were washed 6 times in MABDTr for 15 min each time, and then incubated with Alexa488-conjugated anti-rabbit IgG or Alexa568-conjugated anti-mouse IgG (Molecular Probe; 1:800) at 4 °C overnight. Primary and secondary antibodies were diluted in Can Get Signal immunostain solution A (TOYOBO). After 6 more washings in MABTr, the embryos were whole-mounted on

glass slides and observed with a confocal microscope (LSM 700, Zeiss).

Electron microscopy

For observation using transmission electron microscope (TEM), embryos were dechorionated and fixed at stage 27, 29, 30, 32 or 36 in 100 mM cacodylate buffer (pH 7.4) containing 2% glutaraldehyde and 4% PFA at 4 °C overnight. Samples were post-fixed in 0.06 M s-collidine buffer (pH 7.2) containing 1.3% osmium tetroxide and 0.5% lanthanum nitrate, dehydrated by passage through a graded series of ethanols, and finally embedded in Epon 812 (Taab). Longitudinal sections (120 nm) were stained with 3% uranyl acetate for 20 min and then with 0.4% lead citrate for 5 min. Sections were viewed with a Tecnai Spirit transmission electron microscope (FEI) or a Hitachi H-7100 or H-7650 electron microscope (Hitachi).

For observation using scanning electron microscopy (SEM), embryos were fixed in 0.1 M phosphate buffer (PB, pH 7.4) containing 2.5% glutaraldehyde and 2% PFA. The yolk were removed from the embryo with forceps to expose the heart, and postfixed for 2 h in 1% osmium tetroxide in PB at 4 °C. The embryos were then rinsed in PB, dehydrated in a graded series of ethanol, frozen in t-butyl alcohol, then freeze-dried *in vacuo* with an Eiko ID-2. The embryos were mounted on a metal stub, osmium-coated by using a Filgen OPC60A, and observed with an HS-6 electron microscope (Hitachi).

Muscle relaxation assay

Embryos were incubated with anesthetized in 0.0015% tricaine methanesulfonate in embryo medium for 48 h from stages 27 to 32 to prevent muscle contractions. Treated and untreated embryos were immunostained with F59 antibody obtained from the Developmental Studies Hybridoma Bank at stage 32, and the number of somites with muscle-fiber degeneration was counted.

Results

Enlarged ventricle and muscle disorganization in *zac* mutants

zacro (*zac*) is a recessive, embryonic-lethal mutant obtained by ENU (*N*-ethyl-*N*-nitrosourea) mutagenesis. *zac* mutants were characterized by an abnormally enlarged heart with a gradually reduced blood flow. The normal medaka heart starts to beat at stage 24, and blood flow begins at stage 25. No difference was observed until stage 25 in *zac* embryos; however, by stage 28 prior to the heart looping, *zac* mutants showed blood congestion in the ventricle along with pericardial edema (Figs. 1A, B). Ruptures in the myocardium layer were detected in the *zac* mutants at stage 27, especially in the dorsal-right myocardium of the ventricle (Figs. 1C, D asterisk). As the endocardium was intact in *zac* mutants, we speculate that the blood accumulation was caused by ineffective contraction of the torn myocardium. *zac* mutants appeared to be normal in their somite differentiation during the early stages of somitogenesis; however, by stage 32, they frequently exhibited an abnormal curvature with their tails dorsally up instead of having the normal flat body axis (Figs. 1E, F). We further analyzed the birefringence of myotome muscle of *zac* mutants by using polarized filter microscopy. Birefringency is used to assess muscle organization in zebrafish models of muscle disease (Granato et al., 1996). Wild-type embryos from stage 32 onwards displayed high birefringence due to the ordered array of their myofilaments (Figs. 1G, I), whereas *zac* mutants displayed patchy birefringence at this stage (Fig. 1H), indicating muscle disorganization in some somites. Muscle disorganization in the *zac* mutant continued to progress, and most of the somites lost their birefringence by stage 34 (Fig. 1J). Histological analysis revealed that orientation of each myotube was severely disorganized by stage 40 (Figs. 1K, L).

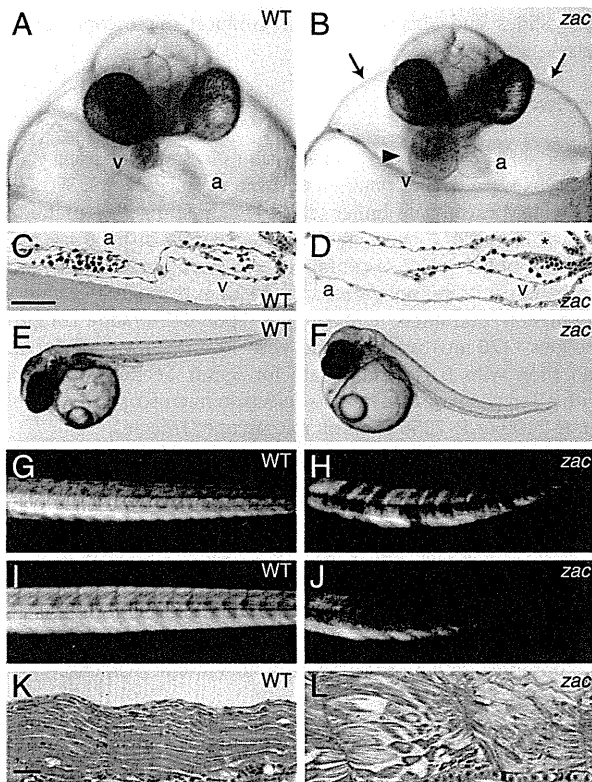


Fig. 1. Cardiac and skeletal muscle phenotypes of *zac* mutants. Embryos from the wild-type (A, C, E, G, I, K) and *zac* mutants (B, D, F, H, J, L). (A, B) Ventricular enlargement in *zac* mutants. Frontal views at stage 28. Dorsal is to the top. Blood cell accumulation in the ventricle (B, arrowhead) and cardiac edema (B, arrows) are visible. a; atrium, v; ventricle (C, D) Hematoxylin and eosin staining of a sagittal section of heart at stage 27. Rostral is to the left. Only the myocardial wall has a rupture (D, asterisk). Scale bar: 20 μ m in "C." (E, F) Whole view from the lateral side at stage 32. *zac* mutants show body curvature. (G–J) Birefringence of skeletal muscle at stage 32 (G, H) and stage 34 (I, J). Rostral is to the left. *zac* mutant shows patchy birefringence at stage 32 and overall reduction in birefringence at stage 34. (K, L) Masson trichrome staining of horizontal sections at stage 32. Rostral is to the right. Striated patterns of sarcomeres can be seen in many muscle cells, but some myofibers have severely degenerated in the *zac* mutants. Scale bar in "K": 20 μ m.

After hatching, *zac* mutants were not able to swim normally, and they died around 14 days post-fertilization. These phenotypes indicate that the *zac* mutation affected both cardiac and skeletal muscles.

Nonsense mutation in *finc* in *zac* mutants

We performed positional cloning to identify the responsible gene in *zac* mutants. By using sequence-tagged site (STS) markers (Kimura et al., 2004), we mapped the *zac* gene to the marker MF01SSA047D04 on the medaka linkage group 6 (Fig. 2A). We searched the expressed sequence tag (EST) markers around the MF01SSA047D04, and found zero and 2 independent recombinants by using AU171271 and O1b2110h, respectively. Therefore, the *zac* gene was placed in the vicinity of AU171271 between MF01SSA047D04 and O1b2110h (Fig. 2A). We further performed fine mapping by utilizing an additional marker, histidine ammonia-lyase (*HAL*), which gave 1 recombinant and narrowed down the *zac* locus. We also found zero recombinants by using another marker, the potassium voltage-gated channel, Shal-related subfamily, member 2 (*KCND2*). Though the genomic sequence encompassing the *zac* locus contained several open reading frames (ORFs), one of them encoded a protein highly homologous to human filamin C, a cardiac and skeletal muscle-specific isoform of the filamin family.

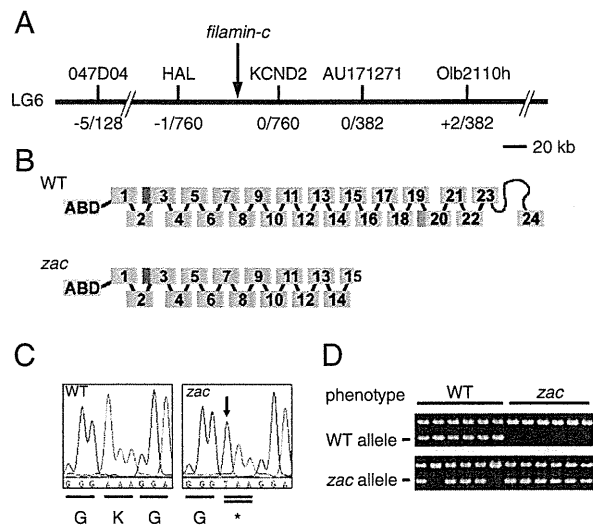


Fig. 2. Positional cloning of *zac* gene (A) Map of the genomic region containing the *zac* gene. The *zac* locus is mapped on the medaka linkage group (LG) 6 by using M-markers, and *finc* is located in the candidate region. HAL, histidine ammonia-lyase and *KCND2*, potassium voltage-gated channel, Shal-related subfamily, member 2. Recombination frequencies for the respective markers are shown below. (B) Schematic drawings of filamin C protein in wild-type and *zac* mutant. The actin-binding domain (ABD) is located at N-terminal followed by 24 repeats of filamin domains. The red region between the 2nd and 3rd repeats indicates the unique splicing variation in medaka fish. The green box between the repeats 19th and 20th is a unique sequence in filamin C members. There is only one hinge sequence between the repeat 23rd and 24th in the medaka filamin C. (C) Chromatogram of the cDNA sequence containing a nonsense mutation from A to T in a coding region of *finc* (arrow). (D) Linkage of *zac* mutation with *finc* as shown by allele-specific genotyping PCR. WT indicates phenotypically wild-type embryos, so some are genotypically heterozygotes revealing both WT and *zac* alleles' PCR products and others are genotypically wild-type having WT allele's PCR product only. All *zac* mutants are genotypically homozygotes, which show the *zac* allele's PCR products only.

The sequence analysis revealed that the medaka *finc* had a high degree of homology (approximately 77% amino acid identity) to the human *FLNC* (Supplementary Fig. 1). The overall structure of medaka filamin C consisted of the actin-binding domain (ABD) and 24 immunoglobulin-like repeats with a hinge region between the 23rd and the 24th repeats (Fig. 2B). Although there was no spacer region between the 15th and the 16th repeats, as found in chicken *FlnC/cgABP260* (Ohashi et al., 2005) and in some human *FLNCs* (Supplementary Fig. 1), the medaka *finc* had a C-isotype-specific insertion sequence between the 19th and the 20th repeats (green box in Fig. 2B; blue underline in Supplementary Fig. 1), which is also seen in mouse *FlnC* (Dalkilic et al., 2006). We also found a novel splicing variation of an additional 39 amino acids between the 2nd and 3rd repeats (red box in Fig. 2B).

We sequenced the entire coding sequence of medaka *finc* from the *zac* mutant and the wild-type sibling alleles and found that the *zac* mutant had a nucleotide substitution from A to T at the first base of codon 1680 (Fig. 2C; AAA to TAA). As a result, this mutation changed the lysine residue to a stop codon (K1680X), causing premature termination in the 15th immunoglobulin-like repeat. This mutation was detected with 100% identity by PCR using allele-specific primers (Fig. 2D).

In the medaka genome database from Ensembl, there is one more filamin C ortholog, which is notated as FLNC (2 of 2). This predicted gene is located mostly in the ultracontig278 and partially in the scaffold698_contig104802. To find the possibility of functional contribution, we examined the sequence similarity of this gene compared to the human filamin C and the medaka filamin C investigated in this study (Supplementary Fig. 2). FLNC (2 of 2) is described as "ol filamin c #3" in this figure. The FLNC (2 of 2) contains 16 filamin-repeats from 9th to 24th repeat of the regular filamin C, and has one hinge region between 23rd and 24th repeat. About three fourth of filamin C-specific region (UR) is pulled out and N-terminal domains of the

actin binding domain and 1–8th repeats are missing. Although the entire sequence is well conserved and the feature of having single hinge represents filamin C, the lack of N-terminal domains is critical. This gene might be termed as “ol fnc 9–24” (Stossel et al., 2001) and functional redundancy would not be expected as for filamin C.

mRNA expression of *fnc* is markedly reduced in *zac* mutants

The pattern of *fnc* expression was analyzed by whole-mount RNA *in situ* hybridization. *fnc* expression was first evident in somites and at the rostral tip of notochord at the onset of somitogenesis. Subsequently, by the 6-somite stage, the expression of *fnc* was detected in the cardiac precursor cells in the anterior lateral-plate mesoderm (Fig. 3A). After migration of the myocardial precursor cells towards the midline, the expression of *fnc* was detected in both the atrium and ventricle (Fig. 3C). These expressions of *fnc* in the somites, the rostral tip of the notochord, and the cardiac muscles continued in subsequent stages (Fig. 3E). At later stages, additional expression was seen in the muscles of the pectoral fin joint and head (data not shown). Although the pattern of expression of *fnc* did not differ between the wild-type and *zac* mutants, the level of expression was reduced in the latter (Figs. 3B, D, F).

To further identify whether this lower expression of *fnc* in *zac* mutants was caused by the transcriptional down-regulation or not,

we generated a transgenic medaka line expressing EGFP under the regulation of a 3 kb-*fnc* promoter. Both in the wild-type and *zac* mutants, the EGFP transgene was expressed at a similar level (Figs. 3G, H), demonstrating that the transcription of the *fnc* gene was not affected by the *zac* mutation. Moreover, the reduced mRNA expression of *fnc* in *zac* mutants was detected before the appearance of abnormal cardiac and muscular phenotypes (Figs. 3A, B), suggesting that the reduction was not caused by any morphological effect in the *zac* mutants. Taken together, these results suggest that the apparently lower expression of *fnc* in *zac* mutants may have been due to the instability of the mutated mRNAs, as often observed in other cases (Baker and Parker, 2004).

To confirm whether the defect in *fnc* was sufficient to cause the *zac* phenotype, we used morpholino antisense oligonucleotides (MO) targeting the translation of *fnc*. When the MO was injected at a dose of 400 μ M, 13% of the injected embryos displayed a *zac*-like cardiac phenotype including the myocardial ruptures ($n=94$; Figs. 3I, J). In contrast to the heart phenotype, we did not observe an abnormal phenotype in the skeletal muscles of the MO-injected embryos. It appears that the MO may have required a longer time before producing the skeletal muscle phenotype, but the effect of MO might not have been strong enough to affect the skeletal muscles. We tested higher concentrations of MO (500–1000 μ M); however, the overall shape of the injected embryos was severely deformed.

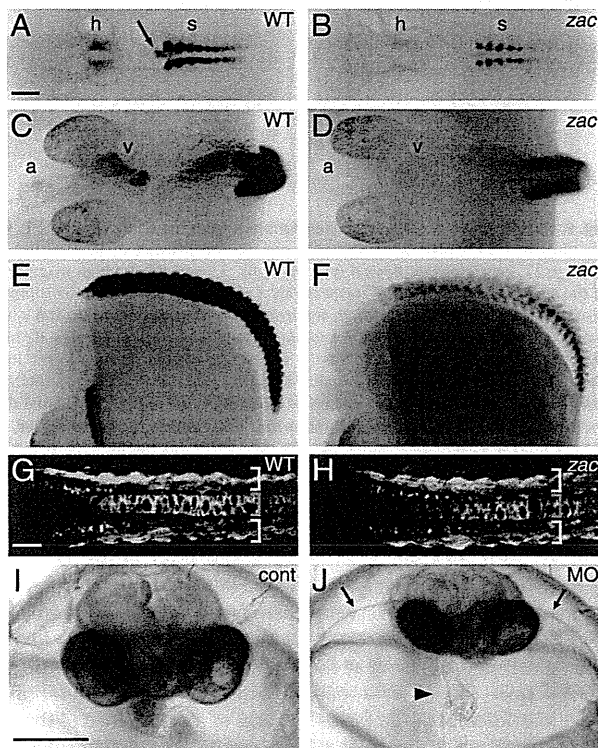


Fig. 3. Expressions of medaka *fnc* in notochord and cardiac and skeletal muscles. Wild-type (A, C, E, G) and *zac* mutant embryos (B, D, F, H). (A–F) Whole-mount RNA *in situ* hybridization analysis of *fnc* expression at stage 22 (A, B) and stage 27 (C–F). Dorsal views (A–D) and lateral views (E, F). Rostral is to the left. *fnc* expression is seen in bilateral cardiac precursor cells (h), somites (s), and the anterior tip of the notochord (arrow). Both atrium (a) and ventricle (v) express *fnc*. Note that *fnc* mRNA expression is reduced in *zac* embryos (B, D, F). (G, H) *fnc* expression visualized in the *fnc* promoter transgenic medaka at stage 26. Dorsal views of the trunk. Rostral is to the left. The level of EGFP expression is not decreased in *zac* mutants, demonstrating that the decrease in the *fnc* mRNAs may be due to instability of mutated *fnc* mRNAs. Yellow and red brackets indicate somites and notochord, respectively. (I, J) Phenocopy by injection of MO. Stage 28, Head frontal views. Dorsal is to the top. Embryos injected with the control MO show the normal appearance (I). However, embryos injected with *fnc*-MO show the cardiac rupture in the ventricle (J: arrowhead) and edema (J: arrows). Scale bars: 100 μ m in “A”, 50 μ m in “G” and 200 μ m in “I”.

zac mutation affects the maintenance of the muscle structure rather than its formation

Since the expression of *fnc* in medaka embryos was detected in the early stage of development (see Fig. 3), we investigated whether the *zac* mutation affected the differentiation of cardiac or skeletal muscle cells by examining the expression of various differentiation marker genes. The expression patterns and levels of cardiac differentiation markers, such as *nlx 2.5*, *tbx5a*, *des*, *cmlc2*, and *vmhc*, were not changed in *zac* hearts at stage 27 (Figs. 4A, B; *cmlc2*, C, D; *des*, the data for *nlx 2.5*, *tbx5a*, and *vmhc* are not shown). The expressions of muscle differentiation markers such as *myoD*, *myf5*, and *des* were also normal in the trunk and tail up to stage 30 (Figs. 4E–H). These results suggest that the early differentiation of cardiac and skeletal muscle cells was not affected in the *zac* mutants.

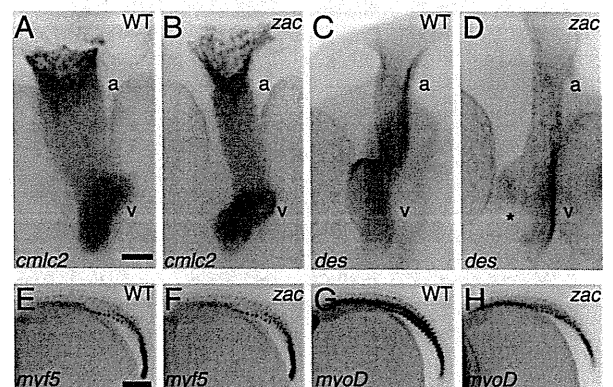


Fig. 4. Expressions of differentiation marker genes in cardiac and skeletal muscle development (A–D). Whole-mount RNA *in situ* hybridization for the expression of cardiomyocyte markers, i.e. *cmlc2* (A, B) and *des* (C, D) at stage 27. Wild-type (A, C) and *zac* mutants (B, D). Dorsal view (A, B) and ventral view (C, D) are shown. Rostral is to the top. Differentiation of cardiomyocytes looks normal. A rupture of the myocardium in the *zac* ventricle is indicated by the asterisk; a: atrium and v: ventricle (E–H). Whole-mount RNA *in situ* hybridization for the expression of muscle markers *myf5* (E, F) and *myoD* (G, H) at stage 27. Wild-type (E, G) and *zac* mutants (F, H). Lateral views. Head is to the left. Both genes show normal expression patterns in the *zac* mutant. Scale bars: 20 μ m in “A” and 200 μ m in “E”.

It has been demonstrated that filamin C protein is localized at the myotendinous junction, Z-disks, and sarcolemma in skeletal muscle fibers, and in the intercalated disks of cardiomyocytes in mammalian and avian hearts (Ohashi et al., 2005; Thompson et al., 2000; van der Ven et al., 2000a). To determine the subcellular localization of filamin C protein in medaka, we performed immunostaining with a filamin C-specific antibody. In the medaka heart, filamin C was localized at cell–cell contact sites between the cardiomyocytes (Fig. 5A). In skeletal muscle, the most abundant expression of filamin C was detected at the junction area where the ends of the muscle fibers attached to the myosepta (Fig. 5B), corresponding to the myotendinous junction (MTJ) in mammals (Summers and Koob, 2002). Filamin C was also localized at the sarcolemma (Figs. 5C–E) and Z-disks (Figs. 5F–H). These results suggest that the localization of filamin C protein is conserved among fish, avians, and mammals.

To examine the effect of filamin C-deficiency on muscle cells, we analyzed *zac* mutants by using a scanning electron microscope (SEM). At stage 27, cardiomyocytes in the *zac* mutant ventricle were not well-ordered ones and had a rougher surface with a number of lamellipodia- and filopodia-like structures (Figs. 6B, D) compared with those in the wild-type heart (Figs. 6A, C), although there was no significant difference in the atrium. These changes were more evident after the onset of blood circulation. Transmission electron microscopic (TEM) analysis of the wild-type heart revealed that organized myofibrils ran along the inner surface side of the cardiomyocytes with the nuclei being located at the outer surface side (Fig. 6E). In contrast, the cytoplasmic structure and subcellular localization of nuclei were severely disorganized in the *zac* mutant (Fig. 6F). Although myofibrils were present even after the rupture of the heart, which is consistent with the fact that the *zac* heart was able to contract, it is also important to note that fewer sarcomere

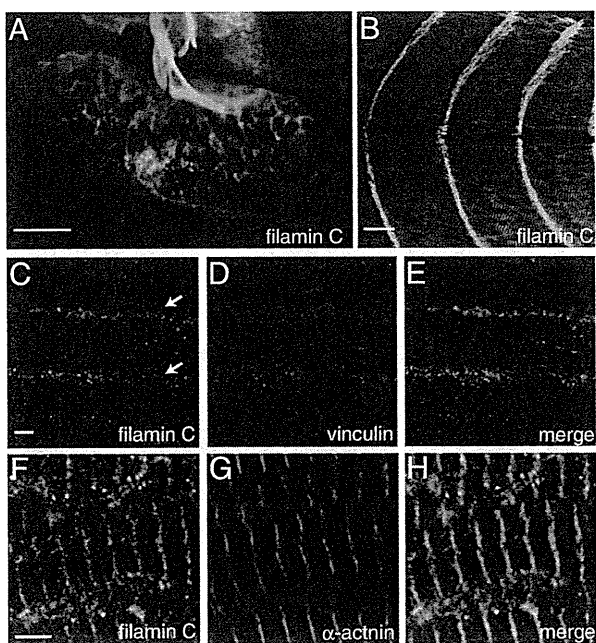


Fig. 5. Subcellular localization of filamin C protein in heart and skeletal muscles. Immunofluorescence staining of filamin C protein in the wild-type embryos. Filamin C is localized at cell–cell contact sites in the heart at stage 32 (A), in the junctional area where the ends of muscle fibers attach to the myosepta (corresponding to myotendinous junction) at stage 32 (B), and in the sarcolemma (C, arrows and merge in “E”), and Z-disks (F and merge in “H”) at stage 40. (C–E) Double staining of filamin C (C), vinculin (D), and their merged image (E). (F–H) Double staining of filamin C (F), α -actinin (G), and their merged image (H). (B–H) Rostral is to the left. Lateral view. Scale bar: 20 μ m in “A” and “B”, 2 μ m in “C” and 4 μ m in “F”.

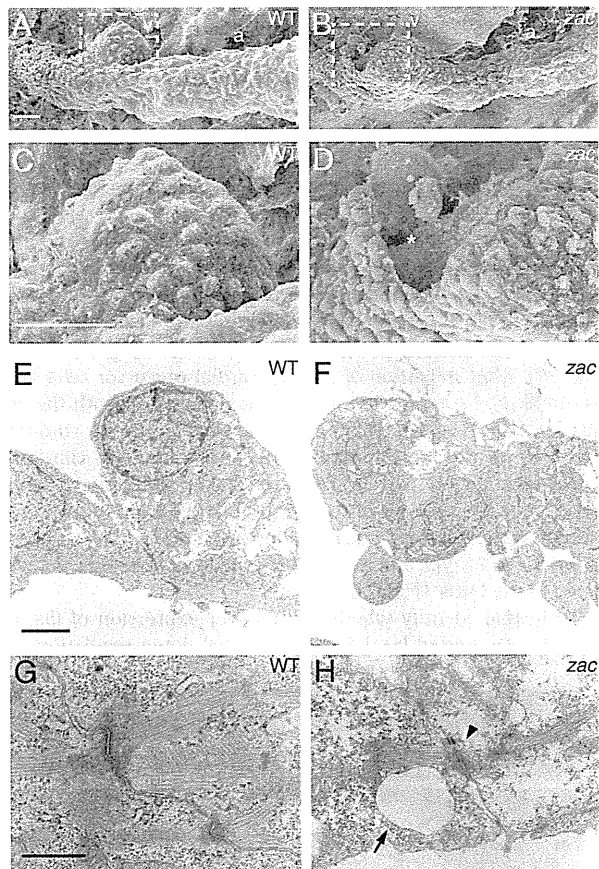


Fig. 6. Ultrastructure of cardiomyocytes. Embryos from the wild-type (A, C, E, G) and *zac* mutants (B, D, F, H). (A–D) Scanning electron microscopic analysis of heart tube at stage 27. Ventral views. Rostral is to the right. “C” and “D” are high magnifications of the boxed area in “A” and “B”, respectively. Cardiomyocytes around the rupture (asterisk) in the *zac* heart show a rough and irregular cell surface. a; atrium and v; ventricle. (E–H) Transmission electron microscopic analysis of cardiomyocytes at stage 27. (E, F) Outer surface of the heart tube is to the top. Cardiomyocytes in *zac* mutants show an abnormal subcellular organization. (G, H) Ultrastructure of intercalated disks at stage 29. Fewer sarcomere bundles are connected to the intercalated disks in *zac* mutants (H, arrowhead) compared with their number in the wild-type (G) at stage 29. Large vacuoles are frequently observed in the *zac* mutants (H, arrow). Scale bar: 20 μ m in “A”, 10 μ m in “C”, 2 μ m in “E” and 1 μ m in “G”.

bundles were attached to the intercalated disks in the *zac* mutants (Figs. 6G, H). Large vacuoles, which contained no sarcoplasmic or membranous materials, were observed in *zac* cardiomyocytes (Fig. 6H). The muscle sarcomere is the important structure for establishing cell–cell adhesion at the intercalated disk between the myocardial cells. Our observations suggest that the *zac* mutation may have interfered with the formation and/or maintenance of the sarcomere structures in the myocardium and that weakened cell–cell adhesion might have resulted in the rupture frequently seen in the ventricle, which is supposed to resist high contraction pressure.

Skeletal muscle was also analyzed by TEM. Although *finc* was expressed from the onset of somitogenesis, the sarcomere structures in the *zac* mutants were normally formed in most of the skeletal muscle fibers and maintained even at stage 30 (Figs. 7A, B). Only in some somites of *zac* mutants had myofibrils degenerated at MTJs at stage 32 (Figs. 7C–F). In addition, focal disorganization of the sarcomere structure was observed in *zac* mutants. In the disorganized area, Z-disks were faint or totally missing (Figs. 7G, H). Many large vacuoles were also observed in *zac* skeletal muscle (Figs. 7I, J). The sarcolemma was frequently detached from the myofibrils, and dilated sarcoplasmic reticula occupied the space between them, in

the *zac* muscle at stage 36 (Figs. 7K, L). These results suggest that filamin C may have contributed to the stabilization of myofibrils at the MTJ, maintenance of the Z-disk structures, and attachment of myofibrils to sarcolemma rather than be involved in myofibril formation.

Reduction in amount of γ -actin at MTJs

Filamins crosslink actin filaments, and link them to cellular membrane by binding to the transmembrane proteins (Stossel et al., 2001). Filamin C interacts with β 1-integrin (Gontier et al., 2005; Loo et al., 1998) and δ/γ -sarcoglycans (Thompson et al., 2000), the components of the DGC. Both complexes are concentrated at MTJs, and have an important role to link subsarcolemmal γ -actin filaments to the ECM in mammals. Since muscle fibers at the MTJs were affected in *zac* mutants, we evaluated the effect of the *zac* mutation on the localization of the proteins involved in this linkage system. Since we did not find any antibodies crossreactive with medaka δ/γ -sarcoglycans, we assessed the sarcoglycan complex by using antibodies against β -sarcoglycan (β -SG). It is known that the entire sarcoglycan complex, containing α -, β -, γ -, and δ -sarcoglycans, becomes destabilized, resulting in decreased localization at the sarcolemma, when any one of its components is disrupted in mammals or zebrafish (Guyon et al., 2005; Mizuno et al., 1994). Similar to the filamin C, integrin β 1D, β -sarcoglycan (β -SG), and γ -actin were accumulated at the MTJ in the wild-type medaka (Fig. 8, upper panels). Although the expressions of integrin β 1D and β -sarcoglycan were not altered in the *zac* mutants, γ -actin was markedly reduced at their MTJs (Fig. 8, lower panels). We also analyzed β -dystroglycan and dystrophin (other components of the DGC) and the phosphorylated forms of FAK and paxillin (downstream molecules of integrin signaling). The results revealed that these molecules were also accumulated at MTJs with no obvious difference in signals between the wild-type and *zac* mutants (data not shown). Since the filamin C is also localized at Z-disks (see Figs. 5F–H), we examined whether the filamin C mutation primarily affected the formation of Z-disks. Double immunostaining of γ -actin and α -actinin revealed that at stage 32 when γ -actin was already altered (Supplementary Fig. 3, upper panels), α -actinin-stained Z-disks were detected normally in *zac* myotome muscle (Supplementary Fig. 3, lower panels), indicating that the primary consequence of the deficiency of filamin C is the defect in the linkage system, not in the Z-disk. These results suggest that filamin C functions to maintain the structural integrity at the MTJs via γ -actin.

zac mutant is more susceptible to mechanical stress by muscle contraction

The observations by electron microscopy and immunohistochemistry demonstrated that muscle degeneration occurred not equally but stochastically in the *zac* mutants. In addition, muscle damage was frequently observed at MTJs, where myofibrils are exposed to strong mechanical stress from muscle contraction. These observations led us to investigate whether muscle degeneration was related to muscle contraction. So we incubated medaka embryos in a solution of tricaine methanesulfonate, which is a common reagent for anesthetizing fish by blocking the action potential. We found that a 0.0015% solution of tricaine methanesulfonate could suppress muscle contraction in medaka embryos without blocking heart beats at stage 27. Under this condition, all embryos survived from stages 27 to 32. So we incubated embryos in this anesthetic and evaluated muscle

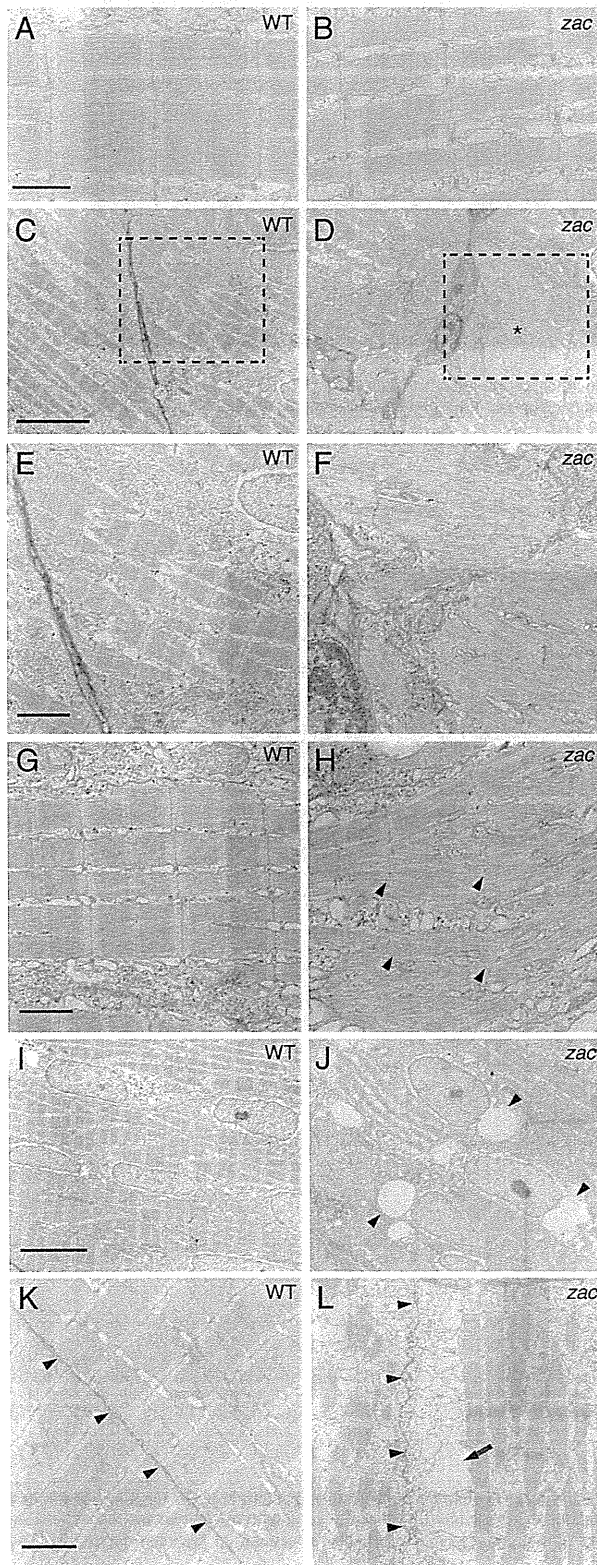


Fig. 7. Ultrastructure of longitudinal section of skeletal muscle. Embryos of wild-type (A, C, E, G, I, K) and *zac* mutant (B, D, F, H, J, L). (A, B) Sarcomere structures are normally formed in *zac* mutants at stage 30. (C–F) Myofibrils have degenerated at myotendinous junctions (asterisk) at stage 32. (E) and (F) are high magnifications of the boxed area in “C” and “D”, respectively. (G, H) Focal disorganization of the sarcomere structure at stage 32. Z-disks are not observed in some myofibrils in *zac* mutants (H, arrowheads). (I, J) Large vacuoles (J, arrowheads) are frequently observed in *zac* mutants at stage 32. They are single-membrane vacuoles, and no sarcomeric or membranous material is seen inside. (K, L) Detachment of sarcolemma from myofibrils in *zac* mutants at stage 36. Even though sarcomere structures are well-preserved, the sarcolemma (arrowheads) has become detached, and dilated sarcoplasmic reticula (L, arrow) occupy the space in *zac* mutants. Scale bar: 1 μ m in “A” and “G”, 5 μ m in “C” and “I” and 2 μ m in “E” and “K”.

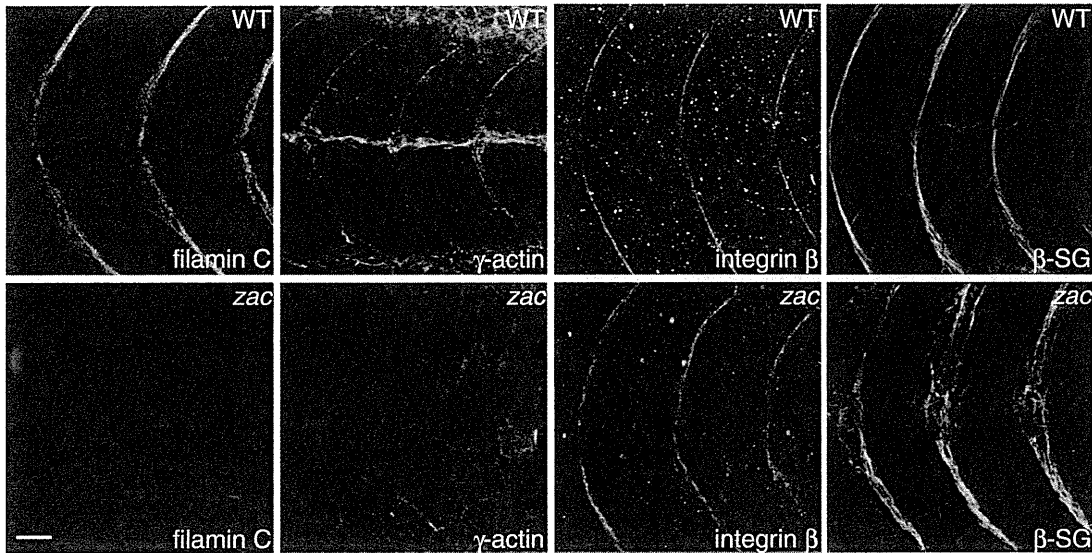


Fig. 8. Immunofluorescence analysis of MTJ. Immunofluorescence stainings of filamin C, γ -actin, integrin β 1D and β -sarcoglycan (β -SG). Each of these proteins accumulates prominently at the MTJ in the wild-type. Only γ -actin protein expression is reduced in the *zac* mutants, whereas other proteins are retained. Rostral is to the left. Stage 32. Scale bar: 20 μ m.

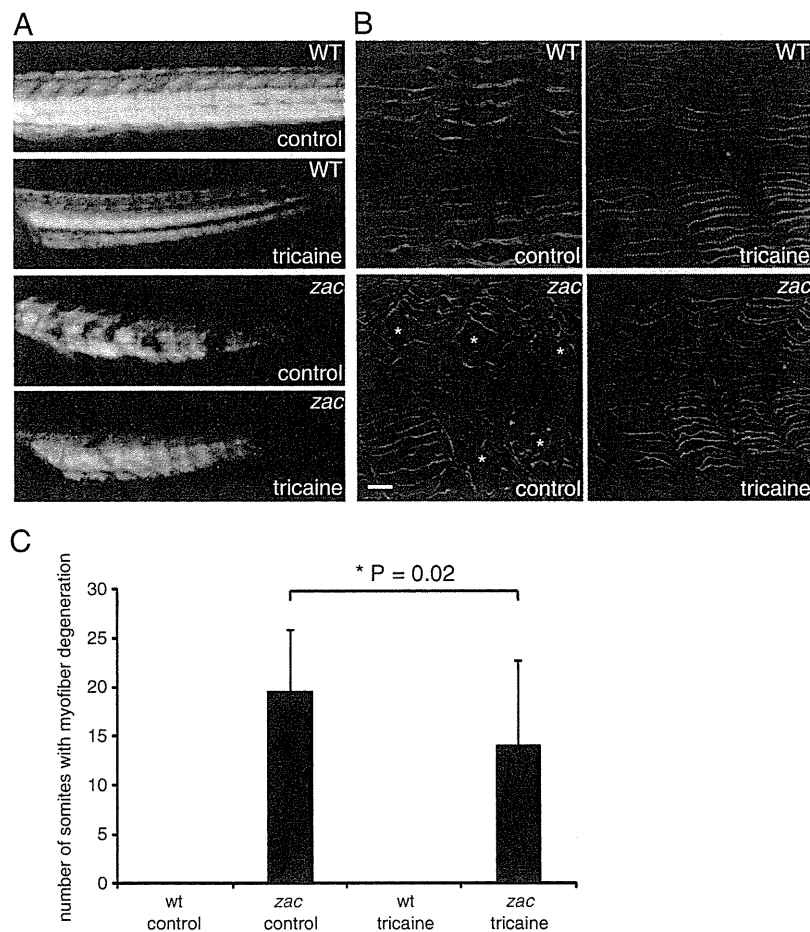


Fig. 9. *zac* mutant is more susceptible to mechanical stress by muscle contraction. (A) Birefringence assay of embryos in the control medium or in the medium containing the anesthetic tricaine methanesulfonate (tricaine). The anesthetized *zac* mutant shows a milder reduction in muscle birefringence compared with the non-treated *zac* mutant. (B) Slow muscle myosin heavy chain staining (F59) of control and anesthetized fish at stage 32. Asterisks show somites having muscle fiber degeneration. Scale bar: 20 μ m. (C) Quantification of muscle degeneration. N = 20, P = 0.02.

degeneration. Anesthetized wild-type embryos appeared to be a bit smaller and skinnier compared with non-treated wild-type embryos, but did not show any perturbed birefringence. As expected, inhibition of locomotion restored muscle birefringence in the *zac* mutants (Fig. 9A). This finding was further confirmed by immunostaining of the slow muscle myosin heavy chain, which staining revealed a decreased level of myofiber disorganization in the anesthetized *zac* mutants (Figs. 9B, C). The myofibers in anesthetized wild-type embryos were thinner than those in the non-treated wild-type embryos, but never had degenerated or become disorganized. Loss of accumulation of γ -actin at the MTJs was not recovered under the tricaine treated condition in the *zac* mutants (data not shown), suggesting that the defect of γ -actin is not contraction-dependent. This is rather supporting the idea that γ -actin is linked to the MTJs by filamin C to reinforce the muscle structure. These results suggest the protective role of filamin C against the mechanical stress to myofibrils caused by muscle contraction.

Discussion

Function of filamin C in the heart

Mutations in human *FLNC* cause a myopathy with altered myofibril organization (Kley et al., 2007; Luan et al., 2010; Shatunov et al., 2009; Vorgerd et al., 2005). These patients frequently show a cardiomyopathy, but the mechanisms causing the cardiac symptom elicited by the each mutation in filamin C have remained unclear. We found that the loss of filamin C in medaka led to cardiac rupture in the ventricular myocardium. Unlike other fish mutants of muscle sarcomere proteins, for example, *pik/ttna* and *sih/tmnt2* (Sehnert et al., 2002; Xu et al., 2002), in which heart beating is severely damaged, the *zac* mutant heart started beating normally, and this beating continued. On the other hand, once the heart beating started, a limited region of the ventricle ruptured, though *flnc* was expressed in all myocardial cells. One reason for this tendency for a limited rupture region is that the ventricle was exposed to higher mechanical stress caused by contraction than was the atrium. Thus, this *zac* mutant phenotype indicates that the loss of filamin C may have weakened the mechanical strength of the heart. In accordance with this notion, we observed that the *zac* cardiomyocytes had an abnormally ruffled cell membrane surface, which is probably a consequence of failure of proper cell–cell adhesion, as previously described in the case of *in vitro* cultured cells (Borm et al., 2005). Moreover, TEM analysis revealed that fewer sarcomere bundles were attached to the intercalated disks, where the muscle sarcomeres are involved in establishing cell–cell adhesion. Based on all of our data taken together, we propose that the function of filamin C in the heart may be required for the integrity and stability of the cardiomyocytes.

Compared with the medaka *zac* mutant, the heart phenotype has not been highlighted in the mouse filamin C-deficient model (Dalkilic et al., 2006). This mouse is designed to generate a partial-loss-of-function model, which lacks only the repeats 20th–24th. The expression of a truncated filamin C was detected in this mouse model, especially at a higher level in heart than in skeletal muscle. Similar truncation mutations in *FLNA* have caused total- or partial-loss-of-function phenotypes in human patients (Feng and Walsh, 2004). Like *FLNA* and *FLNB* mutations (Krakow et al., 2004; Robertson et al., 2003), the position of the mutation may be responsible for variation in the phenotypes in *FLNC*. Recently, Duff et al. reported that mutations in the actin-binding domain of filamin C cause a distal myopathy, in which muscle pathology is totally different from the previous cases having myofibrillar myopathy, which is caused by mutations in either the rod or the dimerization domain of filamin C (Duff et al., 2011). In *zac* mutants, a nonsense mutation in the 15th repeat caused a marked reduction in the level of *flnc* mRNA, such that it was barely detectable in the heart (see Fig. 3F). In addition,

translational knockdown by injecting MO revealed a cardiac phenotype similar to that of the *zac* mutant. Taken together, our present findings indicate that the *zac* mutation may represent complete disruption of the filamin C function, leading to severer phenotypes than those seen in the mouse model.

Function of filamin C in skeletal muscle

Since the expression of filamin C started at the onset of somitogenesis, we examined the effect of the *zac* mutation on muscle differentiation. The expressions of muscle differentiation markers were normal, and most of the muscle fibers showed a completely normal structure, based on the electron microscopic observations made at the early stage. However, muscle degeneration started in focal areas, and progressed, with the result being that a larger area became affected by the hatching stage. This progressive muscle phenotype reminded us of its similarity to the one in filamin C-deficient mice, where most fibers exhibited a normal sarcomeric structure, and only some fibers showed Z-disk abnormality. These results suggest that filamin C plays a role in the maintenance of the muscle structure rather than one in myofibrillogenesis in medaka as well as in mammals.

We observed the accumulation of γ -actin at MTJs in wild-type medaka embryos (see Fig. 8). In mammalian muscle fibers, γ -actin exclusively constitutes the subsarcolemmal actin-based cytoskeleton (Rybakova et al., 2000). The γ -actin filaments provide a structural support to muscle fibers by interacting with DGC and the integrin complex. In medaka embryos, DGC and integrin as well as filamin C were concentrated at the MTJs (Fig. 8). Filamin C interacts with both DGC and integrin (Gontier et al., 2005; Loo et al., 1998; Thompson et al., 2000). It was reported that filamin A, the homologue of filamin C, protects cells from mechanical stress by increasing the rigidity of the cortical actin cytoskeleton in non-muscle cells (D'Addario et al., 2001; D'Addario et al., 2003; Shifrin et al., 2009). Thus, it is most likely that filamin C is involved in the linkage system through its interaction with the actin cytoskeleton, DGC, and integrin at the MTJs. Actually, the γ -actin content was reduced and myofibrils were severely affected at the MTJ in *zac* mutants (Figs. 7D, F and 8). Moreover, sarcomere structures in *zac* mutants were more fragile to mechanical stress caused by muscle contraction (Fig. 9). From these results, we suggest that filamin C participates in the linkage system at the MTJs through the stabilization of γ -actin filaments, protecting sarcomere structures from mechanical stress. In addition, γ -actin is also localized at Z-disks (Nakata et al., 2001), as was filamin C observed presently. Our TEM observation revealed that Z-disks were absent in some myofibrils in the *zac* mutants in late stages and that the sarcolemma had detached from the myofibrils, suggesting another role for filamin C in the lateral connections between myofibrils or between myofibrils and the sarcolemma. Unlike the skeletal muscle, cardiac muscle did not show expression of γ -actin in medaka (data not shown), which is consistent with that γ -actin is expressed mainly in smooth muscle actin (Herman, 1993). Different mechanism and interacting partners with filamin C might be involved to retain the mechanical stability at the intercalated disk in cardiomyocytes.

Patients with mutations in either the rod or the dimerization domain of filamin C show large protein aggregates containing the filamin C itself and its interacting proteins, myotilin and Xin, as well as Z-disk-associated proteins, desmin and α B-crystallin, in the cytoplasm of their muscle fibers (Kley et al., 2007; Luan et al., 2010; Shatunov et al., 2009). Ectopic expression of DGC components in the cytoplasm is also observed. Also, it was demonstrated that the W2710X mutation disturbs the structural stability of filamin C protein, leading to perturbed dimerization (Lowe et al., 2007). As a consequence, it has been suggested that mutant filamin C becomes prone to form aggregates, recruiting its interacting proteins into these aggregates. On the other hand, we did not observe any protein aggregates or cytoplasmic expressions of DGC components in the *zac* mutant. Since the expression of mutant filamin C was remarkably decreased in *zac* mutants, it may have not affected the

localization of the interacting proteins. Instead of aggregates, large vacuoles and dilated sarcoplasmic reticulum were observed electron microscopically in cardiac and skeletal muscle fibers in the *zac* mutants (see Figs. 6H and 7J). These vacuoles, which consisted of a single membrane, did not contain any sarcomeric or membranous materials. These features are totally different from the rimmed vacuoles often seen in patients with the W2710X mutation. Non-rimmed vacuoles with strong PAS-positivity were also reported in these patients, but no accumulation of glycogen was seen in the vacuoles in the *zac* mutants. These vacuoles were not described in the mouse model of filamin C-deficiency, either. Although the presence of vacuoles and dilated sarcoplasmic reticula were described in a report on mechanically induced cell death (Kainulainen et al., 2002) or on animal models of collagen VI-deficiency myopathy, in which apoptosis is enhanced in the skeletal muscle (Irwin et al., 2003; Telfer et al., 2010), the level of apoptosis, as assessed by the TUNEL assay, was not altered in the *zac* mutants (data not shown). Furthermore, no nuclei showing features of apoptosis, such as chromatin condensation, were observed in them. Further studies are required to explain the mechanism of vacuole formation and sarcoplasmic reticulum dilatation.

In light of all of our data taken together, we propose a working hypothesis in which filamin C plays an essential role in maintaining the skeletal and cardiac muscle cell alignment and structure, which hypothesis would explain how these muscles can resist mechanical forces to retain the integrity and stability of their adhesion machineries. Filaminopathy patients frequently develop cardiomyopathy, but the cellular basis for the occurrence of these symptoms has been obscure. Therefore, our analysis using the medaka *zac* mutant offers a useful animal model for understanding the function of filamin C in the maintenance of the structural integrity of muscle cells. Moreover, it has not been proved yet that the function of filamin C is linked to the severe heart phenotype such as the rupture of heart chambers seen in humans. It is possible that filamin C may be associated with idiopathic cardiomyopathy. Further functional analyses may provide us a better understanding of the molecular mechanism of filamin C by which muscular tissues are maintained against mechanical stress.

Finally, regarding the medaka filamin C ortholog: FLNC (2 of 2), to find whether it is involved in Filamin C function in medaka, the further development of medaka genome research is required to confirm the whole genome structure of FLNC (2 of 2).

Supplementary materials related to this article can be found online at doi:10.1016/j.ydbio.2011.10.008.

Acknowledgments

We thank Y. Ishikawa (National Institute for Radiological Sciences, Japan) and members of the screening team for isolating mutants. We thank Y. Takahashi (Iwate Medical University) for heart sectioning and hematoxylin/eosin Y staining, as well as K. Inohaya and Y. Nakatani for their helpful support and discussions. We thank H. Yorifuji (Gunma University Graduate School of Medicine) for providing anti- γ -actin antibody. Hatching enzyme was obtained from National BioResource Project Medaka, Japan. This study was supported by the following sources: a grant-in-aid for scientific research from Japan Society for the Promotion of Science and grants from the programs Research on Psychiatric and Neurological Diseases and Mental Health; Research on Measures for Intractable Diseases; Health Labour Sciences Research Grants for Nervous and Mental Disorders (20B-12, 20B-13) from the Ministry of Health, Labor, and Welfare; and Intramural Research Grants (23-4, 23-5, 23-6) for Neurological and Psychiatric Disorders of NCNP.

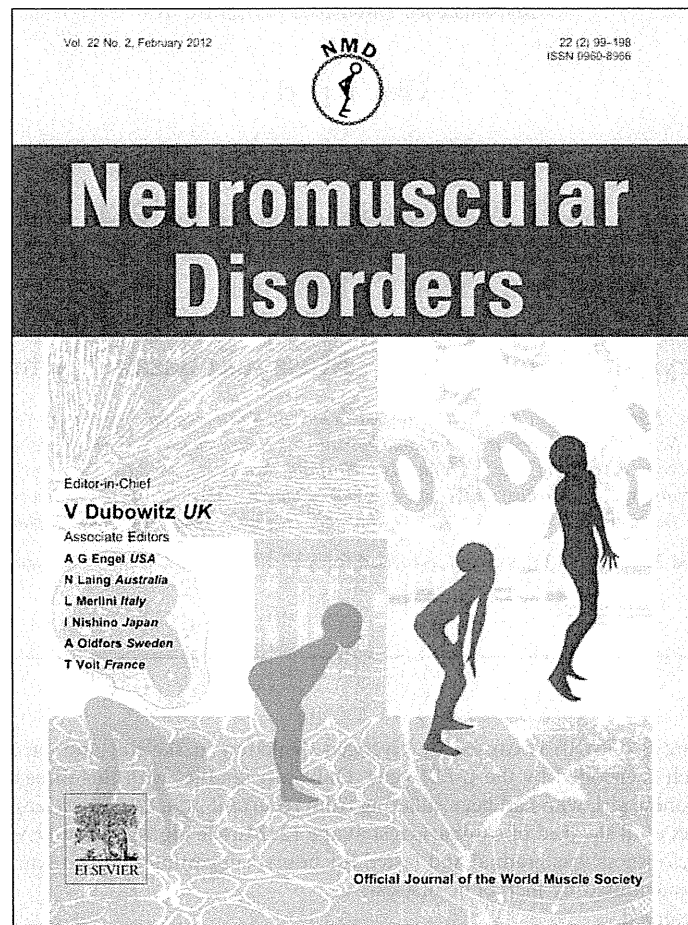
References

Anastasi, G., Cutroneo, G., Gaeta, R., Di Mauro, D., Arco, A., Consolo, A., Santoro, G., Trimarchi, F., Favaloro, A., 2009. Dystrophin-glycoprotein complex and vinculin-talin-integrin system in human adult cardiac muscle. *Int. J. Mol. Med.* 23, 149–159.

- Arahata, K., Ishiura, S., Ishiguro, T., Tsukahara, T., Sahara, Y., Eguchi, C., Ishihara, T., Nonaka, I., Ozawa, E., Sugita, H., 1988. Immunostaining of skeletal and cardiac muscle surface membrane with antibody against Duchenne muscular dystrophy peptide. *Nature* 333, 861–863.
- Baker, K.E., Parker, R., 2004. Nonsense-mediated mRNA decay: terminating erroneous gene expression. *Curr. Opin. Cell Biol.* 16, 293–299.
- Bao, Z.Z., Lakonishok, M., Kaufman, S., Horwitz, A.F., 1993. Alpha 7 beta 1 integrin is a component of the myotendinous junction on skeletal muscle. *J. Cell Sci.* 106, 579–589.
- Bassett, D.I., Bryson-Richardson, R.J., Daggett, D.F., Gautier, P., Keenan, D.G., Currie, P.D., 2003. Dystrophin is required for the formation of stable muscle attachments in the zebrafish embryo. *Development* 130, 5851–5860.
- Bonnemann, C.G., Modi, R., Noguchi, S., Mizuno, Y., Yoshida, M., Gussoni, E., McNally, E.M., Duggan, D.J., Angelini, C., Hoffman, E.P., 1995. Beta-sarcoglycan (A3b) mutations cause autosomal recessive muscular dystrophy with loss of the sarcoglycan complex. *Nat. Genet.* 11, 266–273.
- Borm, B., Requardt, R.P., Herzog, V., Kirfel, G., 2005. Membrane ruffles in cell migration: indicators of inefficient lamellipodia adhesion and compartments of actin filament reorganization. *Exp. Cell Res.* 302, 83–95.
- Burkin, D.J., Kaufman, S.J., 1999. The alpha7beta1 integrin in muscle development and disease. *Cell Tissue Res.* 296, 183–190.
- Campbell, K.P., 1995. Three muscular dystrophies: loss of cytoskeleton-extracellular matrix linkage. *Cell* 80, 675–679.
- Cheng, L., Guo, X.F., Yang, X.Y., Chong, M., Cheng, J., Li, G., Gui, Y.H., Lu, D.R., 2006. Delta-sarcoglycan is necessary for early heart and muscle development in zebrafish. *Biochem. Biophys. Res. Commun.* 344, 1290–1299.
- D'Addario, M., Arora, P.D., Ellen, R.P., McCulloch, C.A., 2003. Regulation of tension-induced mechanotranscriptional signals by the microtubule network in fibroblasts. *J. Biol. Chem.* 278, 53090–53097.
- D'Addario, M., Arora, P.D., Fan, J., Ganss, B., Ellen, R.P., McCulloch, C.A., 2001. Cytoprotection against mechanical forces delivered through beta 1 integrins requires induction of filamin A. *J. Biol. Chem.* 276, 31969–31977.
- Dalkilic, I., Schianda, J., Thompson, T.G., Kunkel, L.M., 2006. Loss of filaminC (FLNC) results in severe defects in myogenesis and myotube structure. *Mol. Cell. Biol.* 26, 6522–6534.
- Duff, R.M., Tay, V., Hackman, P., Ravenscroft, G., McLean, C., Kennedy, P., Steinbach, A., Schoffler, W., van der Ven, P.F., Furst, D.O., Song, J., Djinic-Carugo, K., Penttila, S., Raheem, O., Reardon, K., Malandrini, A., Gambelli, S., Villanova, M., Nowak, K.J., Williams, D.R., Landers, J.E., Brown Jr., R.H., Udd, B., Laing, N.G., 2011. Mutations in the N-terminal actin-binding domain of filamin C cause a distal myopathy. *Am. J. Hum. Genet.* 88, 729–740.
- Ervasti, J.M., 2003. Costameres: the Achilles' heel of Herculean muscle. *J. Biol. Chem.* 278, 13591–13594.
- Faulkner, G., Pallavicini, A., Comelli, A., Salamon, M., Bortoletto, G., Ilevolella, C., Trevisan, S., Kojic, S., Dalla Vecchia, F., Laveder, P., Valle, G., Lanfranchi, G., 2000. FATZ, a filamin-, actinin-, and telethonin-binding protein of the Z-disc of skeletal muscle. *J. Biol. Chem.* 275, 41234–41242.
- Feng, Y., Walsh, C.A., 2004. The many faces of filamin: a versatile molecular scaffold for cell motility and signalling. *Nat. Cell Biol.* 6, 1034–1038.
- Gontier, Y., Taivainen, A., Fontao, L., Sonnenberg, A., van der Flier, A., Carpen, O., Faulkner, G., Borradori, L., 2005. The Z-disc proteins myotilin and FATZ-1 interact with each other and are connected to the sarcolemma via muscle-specific filamins. *J. Cell Sci.* 118, 3739–3749.
- Granato, M., van Eeden, F.J., Schach, U., Trowe, T., Brand, M., Furutani-Seiki, M., Haffter, P., Hamerschmidt, M., Heisenberg, C.P., Jiang, Y.J., Kane, D.A., Kelsch, R.N., Mullins, M.C., Odenthal, J., Nusslein-Volhard, C., 1996. Genes controlling and mediating locomotion behavior of the zebrafish embryo and larva. *Development* 123, 399–413.
- Gupta, V., Kawahara, G., Gundry, S.R., Chen, A.T., Lencer, W.I., Zhou, Y., Zon, L.I., Kunkel, L.M., Beggs, A.H., 2011. The zebrafish *dag1* mutant: a novel genetic model for dystroglycanopathies. *Hum. Mol. Genet.* 20, 1712–1725.
- Guyon, J.R., Mosley, A.N., Jun, S.J., Montanaro, F., Steffen, L.S., Zhou, Y., Nigro, V., Zon, L.I., Kunkel, L.M., 2005. Delta-sarcoglycan is required for early zebrafish muscle organization. *Exp. Cell Res.* 304, 105–115.
- Guyon, J.R., Steffen, L.S., Howell, M.H., Pusack, T.J., Lawrence, C., Kunkel, L.M., 2007. Modeling human muscle disease in zebrafish. *Biochim. Biophys. Acta* 1772, 205–215.
- Hartwig, J.H., Stossel, T.P., 1975. Isolation and properties of actin, myosin, and a new actinbinding protein in rabbit alveolar macrophages. *J. Biol. Chem.* 250, 5696–5705.
- Hayashi, Y.K., Chou, F.L., Engvall, E., Ogawa, M., Matsuda, C., Hirabayashi, S., Yokochi, K., Ziober, B.L., Kramer, R.H., Kaufman, S.J., Ozawa, E., Goto, Y., Nonaka, I., Tsukahara, T., Wang, J.Z., Hoffman, E.P., Arahata, K., 1998. Mutations in the integrin alpha7 gene cause congenital myopathy. *Nat. Genet.* 19, 94–97.
- Herman, I.M., 1993. Actin isoforms. *Curr. Opin. Cell Biol.* 5, 48–55.
- Hoffman, E.P., Brown Jr., R.H., Kunkel, L.M., 1987. Dystrophin: the protein product of the Duchenne muscular dystrophy locus. *Cell* 51, 919–928.
- Hyodo-Taguchi, Y., 1980. Establishment of inbred strains of the teleost, *Oryzias latipes*. *Zool. Mag.* 89, 283–301.
- Inohaya, K., Yasumasu, S., Ishimaru, M., Ohyama, A., Iuchi, I., Yamagami, K., 1995. Temporal and spatial patterns of gene expression for the hatching enzyme in the teleost embryo, *Oryzias latipes*. *Dev. Biol.* 171, 374–385.
- Inohaya, K., Yasumasu, S., Yasumasu, I., Iuchi, I., Yamagami, K., 1999. Analysis of the origin and development of hatching gland cells by transplantation of the embryonic shield in the fish, *Oryzias latipes*. *Dev. Growth Differ.* 41, 557–566.
- Irwin, W.A., Bergamin, N., Sabatelli, P., Reggiani, C., Megighian, A., Merlini, L., Braghetta, P., Columbaro, M., Volpin, D., Bressan, G.M., Bernardi, P., Bonaldo, P., 2003.

- Mitochondrial dysfunction and apoptosis in myopathic mice with collagen VI deficiency. *Nat. Genet.* 35, 367–371.
- Ishikawa, Y., 1996. A recessive lethal mutation, *tb*, that bends the midbrain region of the neural tube in the early embryo of the medaka. *Neurosci. Res.* 24, 313–317.
- Ishikawa, Y., 2000. Medakafish as a model system for vertebrate developmental genetics. *Bioessays* 22, 487–495.
- Ishikawa, Y., Hyodo-Taguchi, Y., Aoki, K., Yasuda, T., Matsumoto, A., Sasanuma, M., 1999. Induction of mutations by ENU in the medaka germline. *Fish Biol. J. Medaka* 10, 27–29.
- Iwamatsu, T., 2004. Stages of normal development in the medaka *Oryzias latipes*. *Mech. Dev.* 121, 605–618.
- Kainulainen, T., Pender, A., D'Addario, M., Feng, Y., Lekic, P., McCulloch, C.A., 2002. Cell death and mechanoprotection by filamin A in connective tissues after challenge by applied tensile forces. *J. Biol. Chem.* 277, 21998–22009.
- Kimura, T., Jindo, T., Narita, T., Naruse, K., Kobayashi, D., Shin, I.T., Kitagawa, T., Sakaguchi, T., Mitani, H., Shima, A., Kohara, Y., Takeda, H., 2004. Large-scale isolation of ESTs from medaka embryos and its application to medaka developmental genetics. *Mech. Dev.* 121, 915–932.
- Kley, R.A., Hellenbroich, Y., van der Ven, P.F., Furst, D.O., Huebner, A., Bruchertseifer, V., Peters, S.A., Heyer, C.M., Kirschner, J., Schroder, R., Fischer, D., Muller, K., Tolksdorf, K., Eger, K., Germing, A., Brodherr, T., Reum, C., Walter, M.C., Lochmuller, H., Ketelsen, U.P., Vorgerd, M., 2007. Clinical and morphological phenotype of the filamin myopathy: a study of 31 German patients. *Brain* 130, 3250–3264.
- Krakow, D., Robertson, S.P., King, L.M., Morgan, T., Sebald, E.T., Bertolotto, C., Wachsmann-Hogiu, S., Acuna, D., Shapiro, S.S., Takafuta, T., Aftimos, S., Kim, C.A., Firth, H., Steiner, C.E., Cormier-Daire, V., Superti-Furga, A., Bonafe, L., Graham Jr., J.M., Grix, A., Bacino, C.A., Allanson, J., Bialer, M.G., Lachman, R.S., Rimoin, D.L., Cohn, D.H., 2004. Mutations in the gene encoding filamin B disrupt vertebral segmentation, joint formation and skeletogenesis. *Nat. Genet.* 36, 405–410.
- Lim, L.E., Duclou, F., Broux, O., Bourg, N., Sunada, Y., Allamand, V., Meyer, J., Richard, I., Moomaw, C., Slaughter, C., Tomé, F.M., Fardeau, M., Jackson, C.E., Beckmann, J.S., Campbell, K.P., 1995. Beta-sarcoglycan: characterization and role in limb-girdle muscular dystrophy linked to 4q12. *Nat. Genet.* 11, 257–265.
- Linnemann, A., van der Ven, P.F., Vakeel, P., Albinus, B., Simonis, D., Bendas, G., Schenk, J.A., Micheel, B., Kley, R.A., Furst, D.O., 2010. The sarcomeric Z-disc component myopodin is a multiadapter protein that interacts with filamin and alpha-actinin. *Eur. J. Cell Biol.* 89, 681–692.
- Loo, D.T., Kanner, S.B., Aruffo, A., 1998. Filamin binds to the cytoplasmic domain of the beta1-integrin. Identification of amino acids responsible for this interaction. *J. Biol. Chem.* 273, 23304–23312.
- Lowe, T., Kley, R.A., van der Ven, P.F., Himmel, M., Huebner, A., Vorgerd, M., Furst, D.O., 2007. The pathomechanism of filaminopathy: altered biochemical properties explain the cellular phenotype of a protein aggregation myopathy. *Hum. Mol. Genet.* 16, 1351–1358.
- Luan, X., Hong, D., Zhang, W., Wang, Z., Yuan, Y., 2010. A novel heterozygous deletion-insertion mutation (2695–2712 del/GTTTGT ins) in exon 18 of the filamin C gene causes filaminopathy in a large Chinese family. *Neuromuscul. Disord.* 20, 390–396.
- Mayer, U., 2003. Integrins: redundant or important players in skeletal muscle? *J. Biol. Chem.* 278, 14587–14590.
- Mayer, U., Saher, G., Fassler, R., Bornemann, A., Echtermeyer, F., von der Mark, H., Miosge, N., Poschl, E., von der Mark, K., 1997. Absence of integrin alpha 7 causes a novel form of muscular dystrophy. *Nat. Genet.* 17, 318–323.
- Miosge, N., Klenczar, C., Herken, R., Willem, M., Mayer, U., 1999. Organization of the myotendinous junction is dependent on the presence of alpha7beta1 integrin. *Lab. Invest.* 79, 1591–1599.
- Mizuno, Y., Noguchi, S., Yamamoto, H., Yoshida, M., Suzuki, A., Hagiwara, Y., Hayashi, Y.K., Arahata, K., Nonaka, I., Hirai, S., Ozawa, E., 1994. Selective defect of sarcoglycan complex in severe childhood autosomal recessive muscular dystrophy muscle. *Biochem. Biophys. Res. Commun.* 203, 979–983.
- Nakata, T., Nishina, Y., Yorifuji, H., 2001. Cytoplasmic gamma actin as a Z-disc protein. *Biochem. Biophys. Res. Commun.* 286, 156–163.
- Naruse, K., Fukamachi, S., Mitani, H., Kondo, M., Matsuoka, T., Kondo, S., Hanamura, N., Morita, Y., Hasegawa, K., Nishigaki, R., Shimada, A., Wada, H., Kusakabe, T., Suzuki, N., Kinoshita, M., Kanamori, A., Terado, T., Kimura, H., Nonaka, M., Shima, A., 2000. A detailed linkage map of medaka, *Oryzias latipes*: comparative genomics and genome evolution. *Genetics* 154, 1773–1784.
- Nigro, V., de Sa Moreira, E., Piluso, G., Vainzof, M., Belsito, A., Politano, L., Puca, A.A., Passos-Bueno, M.R., Zatz, M., 1996. Autosomal recessive limb-girdle muscular dystrophy, LGMD2F, is caused by a mutation in the delta-sarcoglycan gene. *Nat. Genet.* 14, 195–198.
- Noguchi, S., McNally, E.M., Ben Othmane, K., Hagiwara, Y., Yoshida, M., Yamamoto, H., Bornemann, C.G., Gussoni, E., Denton, P.H., Kyriakides, T., Middleton, L., Hentati, F., Ben Hamida, M., Nonaka, I., Vance, J.M., Kunkel, L.M., Ozawa, E., 1995. Mutations in the dystrophin-associated protein gamma-sarcoglycan in chromosome 13 muscular dystrophy. *Science* 270, 819–822.
- Ohashi, K., Oshima, K., Tachikawa, M., Morikawa, N., Hashimoto, Y., Ito, M., Mori, H., Kuribayashi, T., Terasaki, A.G., 2005. Chicken gizzard filamin, retina filamin and cgABP260 are respectively, smooth muscle-, non-muscle- and pan-muscle-type isoforms: distribution and localization in muscles. *Cell Motil. Cytoskeleton* 61, 214–225.
- Postel, R., Vakeel, P., Topczewski, J., Knoll, R., Bakkers, J., 2008. Zebrafish integrin-linked kinase is required in skeletal muscles for strengthening the integrin-ECM adhesion complex. *Dev. Biol.* 318, 92–101.
- Roberts, S.L., Leturcq, F., Allamand, V., Piccolo, F., Jeanpierre, M., Anderson, R.D., Lim, L.E., Lee, J.C., Tomé, F.M., Romero, N.B., Fardeau, M., Beckmann, J.S., Kaplan, J.C., Campbell, K.P., 1994. Missense mutations in the adhalin gene linked to autosomal recessive muscular dystrophy. *Cell* 78, 625–633.
- Robertson, S.P., Twigg, S.R., Sutherland-Smith, A.J., Biancalana, V., Gorlin, R.J., Horn, D., Kenwick, S.J., Kim, C.A., Morava, E., Newbury-Ecob, R., Orstavik, K.H., Quarrell, O.W., Schwartz, C.E., Shears, D.J., Suri, M., Kendrick-Jones, J., Wilkie, A.O., 2003. Localized mutations in the gene encoding the cytoskeletal protein filamin A cause diverse malformations in humans. *Nat. Genet.* 33, 487–491.
- Rybakova, I.N., Patel, J.R., Ervasti, J.M., 2000. The dystrophin complex forms a mechanically strong link between the sarcolemma and costameric actin. *J. Cell Biol.* 150, 1209–1214.
- Samitt, C.E., Bonilla, E., 1990. Immunocytochemical study of dystrophin at the myotendinous junction. *Muscle Nerve* 13, 493–500.
- Sehnert, A.J., Huq, A., Weinstein, B.M., Walker, C., Fishman, M., Stainer, D.Y., 2002. Cardiac troponin T is essential in sarcomere assembly and cardiac contractility. *Nat. Genet.* 31, 106–110.
- Selcen, D., 2008. Myofibrillar myopathies. *Curr. Opin. Neurol.* 21, 585–589.
- Selcen, D., Ohno, K., Engel, A.G., 2004. Myofibrillar myopathy: clinical, morphological and genetic studies in 63 patients. *Brain* 127, 439–451.
- Shatunov, A., Olive, M., Odgerel, Z., Stadelmann-Nessler, C., Irlbacher, K., van Landeghem, F., Bayarsaikhan, M., Lee, H.S., Goudeau, B., Chinnery, P.F., Straub, V., Hilton-Jones, D., Damian, M.S., Kaminska, A., Vicart, P., Bushby, K., Dalakas, M.C., Sambuughin, N., Ferrer, I., Goebel, H.H., Goldfarb, L.G., 2009. In-frame deletion in the seventh immunoglobulin-like repeat of filamin C in a family with myofibrillar myopathy. *Eur. J. Hum. Genet.* 17, 656–663.
- Shifrin, Y., Arora, P.D., Ohta, Y., Calderwood, D.A., McCulloch, C.A., 2009. The role of FilGAP-filamin A interactions in mechanoprotection. *Mol. Biol. Cell* 20, 1269–1279.
- Shimizu, T., Matsumura, K., Sunada, Y., Mannen, T., 1989. Dense immunostainings on both neuromuscular and myotendinous junction with an anti-dystrophin monoclonal antibody. *Biomed. Res.* 10, 405–409.
- Steffen, L.S., Guyon, J.R., Vogel, E.D., Beltre, R., Pusack, T.J., Zhou, Y., Zon, L.I., Kunkel, L.M., 2007. Zebrafish orthologs of human muscular dystrophy genes. *BMC Genomics* 8, 79.
- Stossel, T.P., Condeelis, J., Cooley, L., Hartwig, J.H., Noegel, A., Schleicher, M., Shapiro, S.S., 2001. Filamins as integrators of cell mechanics and signalling. *Nat. Rev. Mol. Cell Biol.* 2, 138–145.
- Stossel, T.P., Hartwig, J.H., 1975. Interactions between actin, myosin, and an actin-binding protein from rabbit alveolar macrophages. Alveolar macrophage myosin Mg²⁺-adenosine triphosphatase requires a cofactor for activation by actin. *J. Biol. Chem.* 250, 5706–5712.
- Summers, A.P., Koob, T.J., 2002. The evolution of tendon — morphology and material properties. *Comp. Biochem. Physiol. A Mol. Integr. Physiol.* 133, 1159–1170.
- Telfer, W.R., Busta, A.S., Bonnemann, C.G., Feldman, E.L., Dowling, J.J., 2010. Zebrafish models of collagen VI-related myopathies. *Hum. Mol. Genet.* 19, 2433–2444.
- Thompson, T.G., Chan, Y.M., Hack, A.A., Brosius, M., Rajala, M., Lidov, H.G., McNally, E.M., Watkins, S., Kunkel, L.M., 2000. Filamin 2 (FLN2): a muscle-specific sarcoglycan interacting protein. *J. Cell Biol.* 148, 115–126.
- van der Flier, A., Gaspar, A.C., Thorsteinsdottir, S., Baudoin, C., Groeneveld, E., Mummery, C.L., Sonnenberg, A., 1997. Spatial and temporal expression of the beta1D integrin during mouse development. *Dev. Dyn.* 210, 472–486.
- van der Ven, P.F., Obermann, W.M., Lemke, B., Gautel, M., Weber, K., Furst, D.O., 2000a. Characterization of muscle filamin isoforms suggests a possible role of gamma-filamin/ABP-L in sarcomeric Z-disc formation. *Cell Motil. Cytoskeleton* 45, 149–162.
- van der Ven, P.F., Wiesner, S., Salmikangas, P., Auerbach, D., Himmel, M., Kempa, S., Hayess, K., Pacholsky, D., Taivainen, A., Schroder, R., Carpen, O., Furst, D.O., 2000b. Indications for a novel muscular dystrophy pathway. gamma-filamin, the muscle-specific filamin isoform, interacts with myotilin. *J. Cell Biol.* 151, 235–248.
- Vorgerd, M., van der Ven, P.F., Bruchertseifer, V., Lowe, T., Kley, R.A., Schroder, R., Lochmuller, H., Himmel, M., Koehler, K., Furst, D.O., Huebner, A., 2005. A mutation in the dimerization domain of filamin c causes a novel type of autosomal dominant myofibrillar myopathy. *Am. J. Hum. Genet.* 77, 297–304.
- Wada, H., Shimada, A., Fukamachi, S., Naruse, K., Shima, A., 1998. Sex-linked inheritance of the If locus in the medaka fish (*Oryzias latipes*). *Zool. Sci.* 15, 123–126.
- Watkins, S.C., Hoffman, E.P., Slayter, H.S., Kunkel, L.M., 1988. Immunoelectron microscopic localization of dystrophin in myofibers. *Nature* 333, 863–866.
- Wittbrodt, J., Shima, A., Scharf, M., 2002. Medaka—a model organism from the far East. *Nat. Rev. Genet.* 3, 53–64.
- Xu, X., Meiler, S.E., Zhong, T.P., Mohideen, M., Crossley, D.A., Burggren, W.W., Fishman, M.C., 2002. Cardiomyopathy in zebrafish due to mutation in an alternatively spliced exon of titin. *Nat. Genet.* 30, 205–209.
- Yoshida, M., Hama, H., Ishikawa-Sakurai, M., Imamura, M., Mizuno, Y., Araishi, K., Wakabayashi-Takai, E., Noguchi, S., Sasaoka, T., Ozawa, E., 2000. Biochemical evidence for association of dystrobrevin with the sarcoglycan-sarcospan complex as a basis for understanding sarcoglycanopathy. *Hum. Mol. Genet.* 9, 1033–1040.

Provided for non-commercial research and education use.
Not for reproduction, distribution or commercial use.



This article appeared in a journal published by Elsevier. The attached copy is furnished to the author for internal non-commercial research and education use, including for instruction at the authors institution and sharing with colleagues.

Other uses, including reproduction and distribution, or selling or licensing copies, or posting to personal, institutional or third party websites are prohibited.

In most cases authors are permitted to post their version of the article (e.g. in Word or Tex form) to their personal website or institutional repository. Authors requiring further information regarding Elsevier's archiving and manuscript policies are encouraged to visit:

<http://www.elsevier.com/copyright>

Case report

Muscle glycogen storage disease 0 presenting recurrent syncope with weakness and myalgia

Sayuri Sukigara^a, Wen-Chen Liang^{b,c}, Hirofumi Komaki^a, Tokiko Fukuda^d, Takeshi Miyamoto^e, Takashi Saito^a, Yoshiaki Saito^a, Eiji Nakagawa^a, Kenji Sugai^a, Yukiko K. Hayashi^b, Hideo Sugie^d, Masayuki Sasaki^a, Ichizo Nishino^{b,*}

^a Department of Child Neurology, National Center Hospital, National Center of Neurology and Psychiatry (NCNP), Kodaira, Tokyo, Japan

^b Department of Neuromuscular Research, National Institute of Neuroscience, NCNP, Kodaira, Tokyo, Japan

^c Department of Pediatrics, Kaohsiung Medical University Hospital, Kaohsiung Medical University, Kaohsiung, Taiwan

^d Department of Pediatrics, Jichi Medical University and Jichi Children's Medical Center, Shimotsuke, Tochigi, Japan

^e Department of Pediatrics, Kosai Municipal Hospital, Kosai, Shizuoka, Japan

Received 22 March 2011; received in revised form 17 June 2011; accepted 22 August 2011

Abstract

Muscle glycogen storage disease 0 (GSD0) is caused by glycogen depletion in skeletal and cardiac muscles due to deficiency of glycogen synthase 1 (GYS1), which is encoded by the *GYS1* gene. Only two families with this disease have been identified. We report a new muscle GSD0 patient, a Japanese girl, who had been suffering from recurrent attacks of exertional syncope accompanied by muscle weakness and pain since age 5 years until she died of cardiac arrest at age 12. Muscle biopsy at age 11 years showed glycogen depletion in all muscle fibers. Her loss of consciousness was gradual and lasted for hours, suggesting that the syncope may not be simply caused by cardiac event but probably also contributed by metabolic distress.

© 2011 Elsevier B.V. All rights reserved.

Keywords: Glycogen storage disease; Glycogen synthase; Glycogen; Syncope; Sudden death

1. Introduction

Glycogen is a high molecular mass polysaccharide that serves as a repository of glucose for use in times of metabolic need. It is stored in liver, cardiac and skeletal muscles, and broken down to glucose to produce ATP as energy as needed. For the synthesis of glycogen, at least two proteins, glycogenin (GYG) and glycogen synthase (GYS), are known to be essential. GYG is involved in the initiation reactions of glycogen synthesis: the covalent attachment of a glucose residue to GYG is followed by elongation to

form an oligosaccharide chain [1]. GYS catalyzes the addition of glucose monomers to the growing glycogen molecule through the formation of alpha-1,4-glycoside linkages [2].

Defect in either GYG or GYS can cause glycogen depletion. Recently, muscle glycogen deficiency due to a mutation in a gene encoding muscle GYG, *GYG1*, was reported [3] and named as glycogen storage disease type XV. In contrast, glycogen depletion caused by the *GYS* gene mutation is called glycogen storage disease type 0 (GSD0). GSD0 was first reported in 1990 in patients with type 2 diabetes who had a defect in glycogen synthesis in liver, which was caused by a defect in liver GYS, *GYS2*, and the disease was named as liver GSD0 (or also called GSD0a) [4,5].

The disease of muscle GYS, *GYS1*, was first described in 2007 in three siblings and named muscle GSD0, which is

* Corresponding author. Address: Department of Neuromuscular Research, National Institute of Neuroscience, NCNP, 4-1-1, Ogawahigashi-cho, Kodaira, Tokyo 187 8551, Japan. Tel.: +81 42 3412711; fax: +81 42 3427521.

E-mail address: nishino@ncnp.go.jp (I. Nishino).

also called GSD0b [6]. One of the patients initially manifested exercise intolerance, epilepsy and long QT syndrome since the age of 4 years, then died of sudden cardiac arrest after exertion when he was 10.5-year-old. The other two siblings were then genetically confirmed as muscle GSD0 with mutations in *GYS1* and cardiac involvement was also found in both. The second muscle GSD0 family was reported in 2009 [7]. The 8-year-old boy had been healthy before collapsing during a bout of exercise, resulting in death. Post-mortem examinations and studies verified the diagnosis of muscle GSD0. He had a female sibling who died at 6 days of age of undetermined cause. Here we report the first muscle GSD0 patient in Asia with some distinct clinical manifestations from other reported cases.

2. Case report

An 11-year-old Japanese girl with repeated episodes of post-exercise loss of consciousness, weakness, and myalgia since age 5 years, was admitted to the hospital. She was the first child of unrelated healthy parents. She was born uneventfully and was normal in psychomotor development. At age 2 years, she developed the first episode of generalized tonic-clonic seizure while she was sleeping. At age 4 years, she had the second episode of generalized tonic-clonic seizure when she was under general anesthesia for tonsillectomy, whose cause was thought to be hypoglycemia due to prolonged fasting. In both episodes, seizure was followed by strong limb pain. At age 5 years, she suffered from the first episode of syncope while climbing up stairs. She recovered after a few hours. One year later, she had the second syncopal attack after running 50 m, which was accompanied by subsequent limb muscle weakness and myalgia. Since then, similar episodes were repeated several times a year. For each bout, she first developed leg muscle weakness immediately after exercise, making her squat down, and gradually lost the consciousness. She recovered her consciousness after a few hours but always experienced strong myalgia in legs which lasted for several hours. Blood glucose level was not decreased during these attacks.

On admission, general physical examination revealed no abnormal finding. On neurological examination, she had mild proximal dominant muscle weakness and mildly limited dorsiflexion of both ankle joints. T1-weighted images of skeletal muscle MRI showed high signal intensities in gluteal and flexor muscles of the thigh, which were assessed to be fatty degeneration (Fig. 1). Systemic investigations including electrocardiography, echocardiography, stress cardiac catheterization, stress myocardial scintigraphy, brain imaging, electroencephalography, and screening tests for metabolic diseases revealed no abnormality except for a mild ischemic finding on exercise electrocardiography. Ischemic and non-ischemic forearm exercise tests [8] showed the lack of lactate elevation, raising a possibility of glycogen storage disease. A few months later, resting electrocardiography, 24-h holter monitoring and resting echocardiography were re-evaluated and again revealed normal findings.

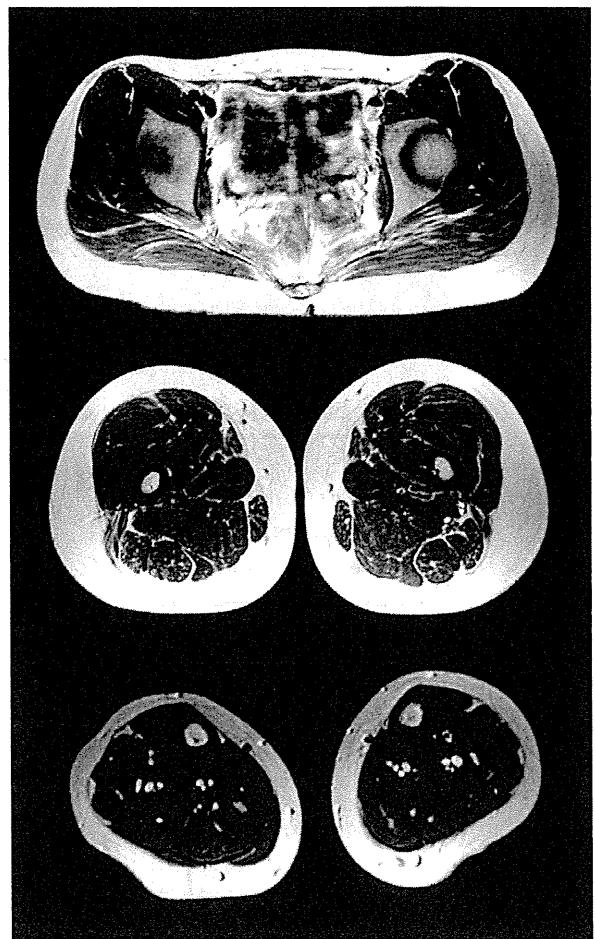


Fig. 1. Muscle MRI, T2WI, axial. It shows high intensity in gluteus maximus and biceps femoris muscles.

3. Histological analysis of skeletal muscle

Muscle biopsy was performed from biceps brachii. Serial frozen sections were stained with hematoxylin and eosin, modified Gomori trichrome, and a battery of histochemical methods. The most striking finding was depletion of glycogen in all muscle fibers but not in the interstitium on periodic acid-schiff (PAS) staining (Fig. 2A). Phosphorylase activity was also deficient in all fibers (Fig. 2B). Mitochondria especially at the periphery of muscle fibers were prominent on modified Gomori trichrome (Fig. 2D). ATP-ase staining revealed type 2 fiber atrophy. Electron microscopic analysis showed mitochondrial proliferation at the periphery of muscle fibers with no notable intramitochondrial inclusions (Fig. 2E).

4. Biochemical and molecular analysis

Both the activity of *GYS1* and the amount of glycogen in the skeletal muscle were markedly reduced (Table 1). On western blotting, *GYS1* in the patient's skeletal muscle was undetectable (Fig. 2F). The *GYS1* gene sequence analysis revealed compound heterozygous mutation of

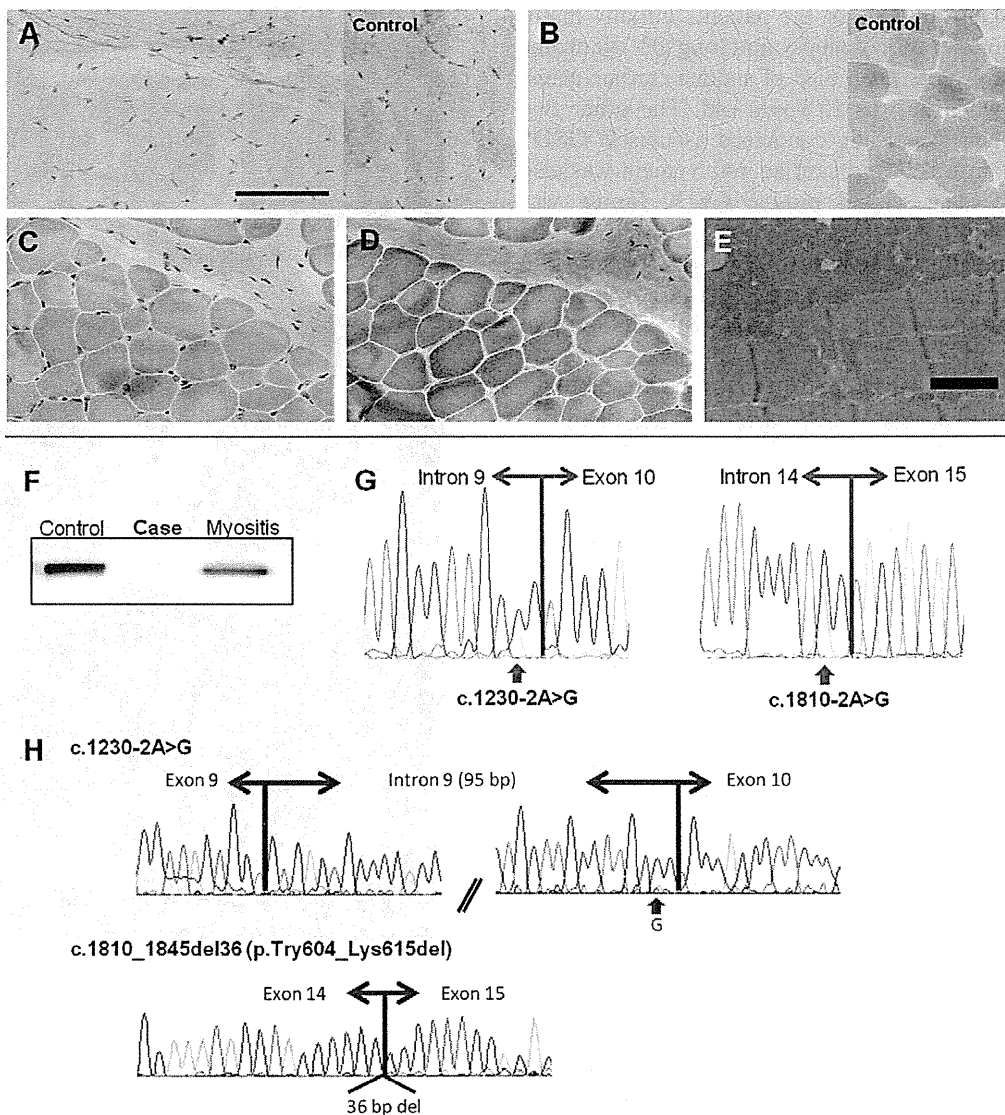


Fig. 2. Histological, genetic and protein analyses. Periodic acid-schiff (PAS) staining shows marked depletion of glycogen in muscle fibers but not in the interstitium (A). Phosphorylase activity is also deficient in all fibers (B). Hematoxylin and eosin staining shows mild fiber size variation (C). On modified Gomori trichrome, mitochondria are prominent especially at the margin of each muscle fiber (D). On electron microscopy (EM), mitochondria are increased in number at the periphery of muscle fibers (E). Bars represent 100 μ m for histochemistry and 7 μ m for EM. On western blotting using anti-GYS1 antibody (Abcam), GYS1 protein is absent in skeletal muscle from the patient (F). Sequence analysis for the *GYS1* gene reveals a compound heterozygous mutation of c.1230-2A>G and c.1810-2A>G (G). cDNA analysis showed insertion of intron 9 between exon 9 and 10 and 36-bp deletion from the beginning of exon 15 (H).

Table 1

Analyses of enzymatic activity and glycogen content. The activity of GYS and glycogen content in skeletal muscle were markedly reduced.

	Glycogen synthase (mol/min/mg)	UDPG-pyrophosphorylase (nmol/min/mg)	Glycogen contents (% of wet weight)
Patient	<i>0.9</i>	30.5	<i>0.03</i>
Control	42.0 \pm 11.2	31.2 \pm 3.5	0.94 \pm 0.55

Italicized values: lower than control range.

c.1230-2A>G in intron 9 and c.1810-2A>G in intron 14 (Fig. 2G). cDNA analysis confirmed the insertion of the full-length intron 9 between exons 9 and 10 and a 36-bp deletion in the beginning of exon 15 (Fig. 2H).

5. Clinical course after diagnosis

Upon the diagnosis of GSD0, exercise was strictly limited to avoid syncope resulted from glucose depletion. In

addition, oral intake of cornstarch (2 g/kg, every 6 h) was started to maintain blood sugar level. Her condition had been stable for 1 year after diagnosis. However, at age 12 years, she was found lying unconsciously on the stairs at her school. She had persistent asystole despite ambulance resuscitation. The blood glucose level in the emergency room was above 100 mg/dl.

6. Discussion

We identified the first Asian patient with muscle GSD0, who manifested recurrent episodes of syncope with subsequent muscle weakness and myalgia, and eventually developed cardiac arrest.

Findings in our patient seem to be similar to previous reports, but some differences indicated the possibility of another pathogenesis of the disease. Our patient repeatedly suffered from episodes of syncope. In contrast to two earlier reports, those patients never had syncope, although the last attack led to sudden death [6,7]. In support of this notion, most muscle glycogen synthase knock-out mice died soon after birth due to impaired cardiac function [8]. However, the pattern of loss of consciousness in our patient cannot be explained by simple cardiac dysfunction, as she lost her consciousness gradually after exercise and took hours to regain, which is different from typical cardiac syncope, usually showing sudden loss of consciousness and rapid recovery. Alternatively, defective glycogen synthesis in brain may be related to syncope, as *GYS1* is also expressed in brain, albeit not so much as in cardiac and skeletal muscles. Another possibility may be intermittent arrhythmia. However, electrocardiogram during the episode was never obtained. Further studies are necessary to answer this question.

On muscle pathology and electron microscopy, we found profound deficiency of glycogen in all muscle fibers accompanied by mitochondrial proliferation, which is similar to previous reports. The mitochondrial proliferation may reflect a compensatory mechanism for supplying ATP to glycogen-depleted muscles. Interestingly, phosphorylase activity on histochemistry seemed deficient. This is consistent with the fact that endogenous glycogen is used as a substrate of phosphorylase on histochemistry. Previous reports described the reduced number of type 2 fibers. In our patient, type 2 fiber atrophy, but not type 2 fiber deficiency, was seen. Although type 2 fiber atrophy is a nonspecific finding, this picture might also reflect the dysfunction of glycogen-dependent muscle fibers.

7. Conclusion

We identified the first Asian patient with muscle GSD0. In our patient, recurrent episodes of syncope and eventual sudden death may not be simply explained by cardiac dysfunction. Further studies are necessary to elucidate the mechanism of syncope in muscle GSD0 and to establish appropriate guideline of management for these patients to prevent sudden death.

Acknowledgments

The authors thank Ms. Goto and Ms. Ogawa (National Center of Neurology and Psychiatry) for technical assistance in mutation analysis. This work is supported by: a Grant-in-Aid for Scientific Research from Japan Society for the Promotion of Science; Research on Psychiatric and Neurological Diseases and Mental Health, Research on Measures for Intractable Diseases, Health Labour Sciences Research Grant for Nervous and Mental Disorders (20B-12, 20B-13) from the Ministry of Health, Labor, and Welfare, and Intramural Research Grant (23-4, 23-5, 23-6) for Neurological and Psychiatric Disorders of NCNP.

References

- [1] Viskupic E, Cao Y, Zhang W, Cheng C, DePaoli-Roach AA, Roach PJ. *J Biol Chem* 1992;267:25759–63.
- [2] Pederson BA et al. Abnormal cardiac development in the absence of heart glycogen. *Mol Cell Biol* 2004;24:7179–87.
- [3] Moslemi AR, Lindberg C, Nilsson J, Tajsharghi H, Andersson B, Oldfors A. Glycogenin-1 deficiency and inactivated priming of glycogen synthesis. *N Eng J Med* 2010;362:1203–10.
- [4] Shulman GI, Rothman DI, Jue T, Stein P, DeFronzo PA, Shulman RG. Quantitation of muscle glycogen synthesis in normal subjects and subjects with non-insulin-dependent diabetes by ¹³C nuclear magnetic resonance spectroscopy. *N Eng J Med* 1990;322:223–8.
- [5] Orho M, Bosshard NU, Buist NR, Gitzelmann R, Aynsley-Green A, Blümel P, et al. Mutations in the liver glycogen synthase gene in children with hypoglycemia due to glycogen storage disease type 0. *J Clin Invest* 1998;102:507–15.
- [6] Kollberg G, Tulinius M, Gilljam T, Ostman-Smith I, Forsander G, Jotorp P, et al. Cardiomyopathy and exercise intolerance in muscle glycogen storage disease 0. *N Engl J Med* 2007;357:1507–14.
- [7] Cameron JM, Levandovskiy V, MacKay N, Utgiker R, Ackerley C, Chiasson D, et al. Identification of a novel mutation in *GYS1* (muscle-specific glycogen synthase) resulting in sudden cardiac death, that is diagnosable from skin fibroblasts. *Mol Genet Metab* 2009;98:378–82.
- [8] Pederson BA, Cope CR, Schroeder JM, Smith NW, Irimia JM, Thurberg BL, et al. Exercise capacity of mice genetically lacking muscle glycogen synthase: in mice, muscle glycogen is not essential for exercise. *J Biol Chem* 2005;280:17260–5.

Increase in number of sporadic inclusion body myositis (sIBM) in Japan

Naoki Suzuki · Masashi Aoki ·
Madoka Mori-Yoshimura · Yukiko K. Hayashi ·
Ikuya Nonaka · Ichizo Nishino

Received: 28 May 2011 / Accepted: 12 July 2011 / Published online: 29 July 2011
© Springer-Verlag 2011

Dear Sirs,

Sporadic inclusion body myositis (sIBM) is the most common form of myopathy with inflammation in those over the age of 50 years in Western countries [1, 3, 5, 7]. The prevalence in Caucasians is 4.9–14.9 per million, but 1.07 in Turkey [6]. The prevalence of sIBM in Asian people including Japanese has not been examined. Several mechanisms of sIBM are proposed, for example, beta-amyloid accumulation, immune system abnormalities, viral infection, genetic background [1, 8]. However, none of these are concluded to be the specific cause of sIBM.

We have now performed a retrospective survey of Japanese patients of sIBM diagnosed at the National Center of Neurology and Psychiatry (NCNP). The increasing numbers of sIBM patients may suggest the clue to elucidate the pathomechanism of sIBM.

Only patients with ‘definite’ or ‘probable’ sIBM by the clinical and biopsy criteria [7] were included in the analysis. Biopsies were re-evaluated, and were confirmed the pathological diagnosis of sIBM. We also used revised Bohan and Peter criteria for diagnosis of polymyositis (PM) [5]. In NCNP, the first patient of sIBM was diagnosed in 1989, and the number of patients diagnosed has been increasing year by year, especially after 2002 (Fig. 1). A total of 77 sIBM patients were identified between 1990 and 2007. The average age of onset in sIBM in Japan was 63.4 years old. The numbers of patients with sIBM and PM between 1999 and 2007 were 69 and 165, respectively (Table 1). Accordingly, the number of sIBM patients is estimated to be half that of PM. Given the number of PM patients in the national survey in 2003 (approximately 3,000 patients) in Japan, the number of sIBM is estimated to be around 1,250. Therefore, we assess that the prevalence of sIBM in Japan is 9.83 per million in 2003. The numbers of sIBM and PM between 1990 and 1998 were 8 and 151 patients, respectively. As the number of PM patients in the national survey of 1991 was still around 3,000, the prevalence calculated by the same method was 1.28 per million in 1991, suggesting an increase in the number of sIBM in Japan. We also examined the relationship between birth year and the number of sIBM patients diagnosed in NCNP since 1978 (Fig. 1b). The numbers of sIBM patients are increasing in a linear manner among the individuals born after 1920s.

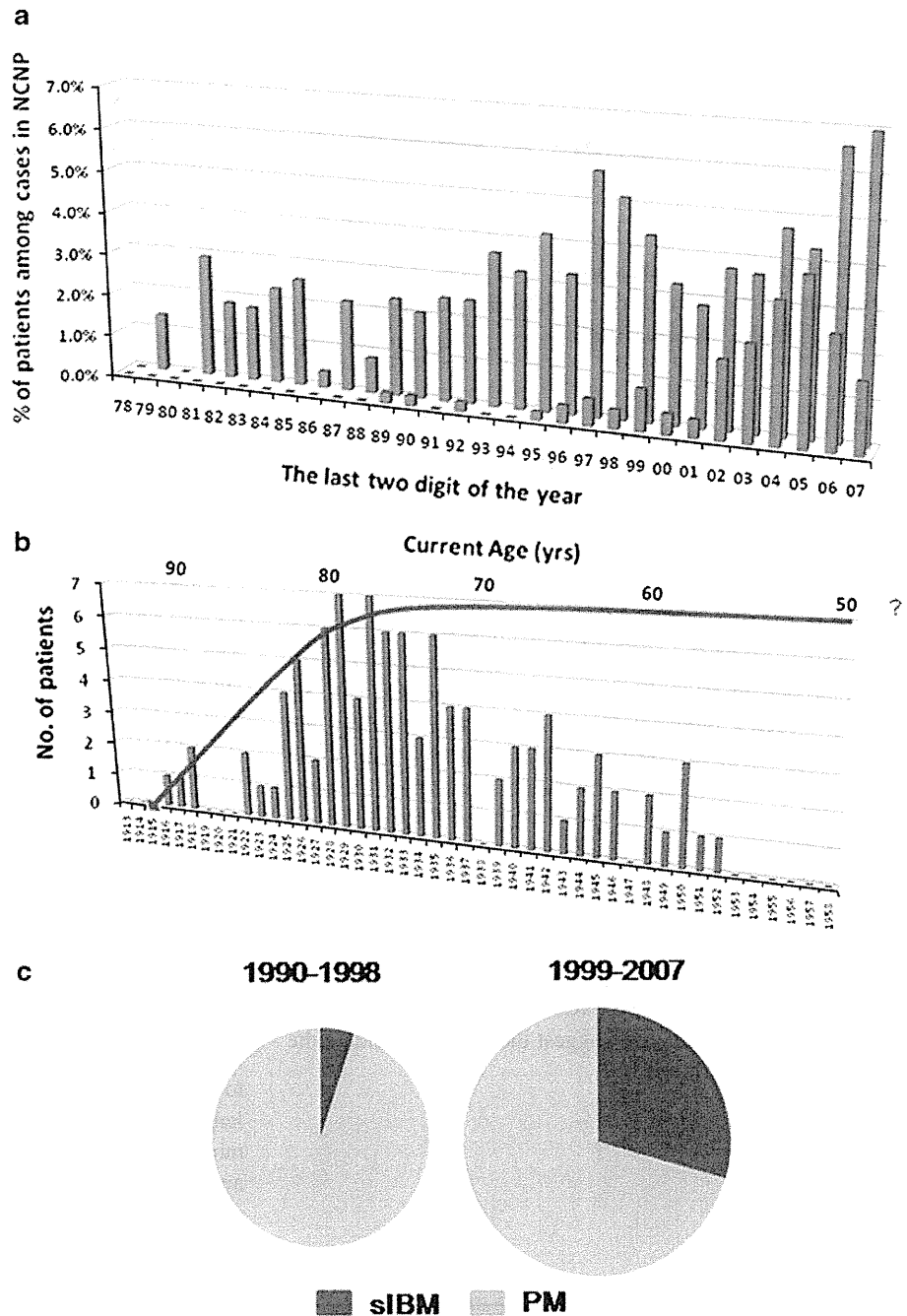
The etiology of sIBM is not yet known and still under discussion in either a primary inflammatory myopathy or a primary degenerative myopathy with a secondary inflammatory disease. The lack of significant clinical response with various immunosuppressants is against sIBM being a primary autoimmune disorder. Accumulation of beta-amyloid in rimmed vacuoles is interpreted as a primary

N. Suzuki · M. Aoki (✉)
Department of Neurology, Tohoku University School
of Medicine, 1-1Seiryō-machi, Aoba-ku,
Sendai 980-8574, Japan
e-mail: aokim@med.tohoku.ac.jp

M. Mori-Yoshimura
Department of Neurology, National Center of Neurology
and Psychiatry (NCNP), Tokyo, Japan

Y. K. Hayashi · I. Nonaka · I. Nishino
Department of Neuromuscular Research, National Institute
of Neuroscience, National Center of Neurology
and Psychiatry (NCNP), Tokyo, Japan

Fig. 1 a The number of IBM patients diagnosed in NCNP is increasing year by year. The blue bar represents the percentage of patients with polymyositis (PM) and the red bar represents sporadic inclusion body myositis (sIBM). **b** The relationship between the birth year and the number of sIBM patients diagnosed in NCNP since 1978. The vertical axis represents the number of sIBM patients. Note that the persons born after 1940s are now in their sixties and are at the optimal disease onset of age for sIBM. **c** The number of sIBM and PM patients diagnosed in the NCNP. Data are presented as the total of each half decade



degenerative mechanism [2]; however, some researcher pointed out that beta-amyloid is not specifically found with immunohistochemistry [9]. It was previously reported that two out of six female rabbits fed a cholesterol-enriched diet presented pathological features resembling sIBM [4]. As observed in our study, we found many patients diagnosed after 2002. The age at onset of sIBM is around 60 years old [7]. Interestingly, patients born after the 1940s were in their sixties in the 2000s and were at the optimal age of disease

onset for sIBM. The increasing numbers of sIBM is followed by the rapid change of dietary habit from traditional style to a Westernized one after World War II in Japan. These data suggest that the change of dietary habit may have an influence on the increasing number of sIBM patients in Japan.

It is needed to consider the influence of prolongation of life span in Japan and also the presence of a referral filter bias for diagnostically difficult patients. Diagnostic